Journal of Ovarian Research

RESEARCH

Open Access

Bone marrow mesenchymal stem cells expressing Neat-1, Hotair-1, miR-21, miR-644, and miR-144 subsided cyclophosphamide-induced ovarian insufficiency by remodeling the IGF-1–kisspeptin system, ovarian apoptosis, and angiogenesis

Amany I. Ahmed[1], Mohamed F. Dowidar[1], Asmaa F. Negm[1], Hussein Abdellatif[2,3], Asma Alanazi[4,5], Mohammed Alassiri[5,6], Walaa Samy[7], Dina Mohamed Mekawy[8,9], Eman M. A. Abdelghany[10], Nesma I. El-Naseery[11], Mohamed A. Ibrahem[12], Emad Ali Albadawi[13], Wed Salah[14], Mamdouh Eldesoqui[15,16], Emil Tîrziu[17], Iulia Maria Bucur[17*], Ahmed Hamed Arisha[18,19*] and Tarek Khamis[20*]

Abstract

Ovarian insufficiency is one of the common reproductive disorders affecting women with limited therapeutic aids. Mesenchymal stem cells have been investigated in such disorders before yet, the exact mechanism of MSCs in ovarian regeneration regarding their epigenetic regulation remains elusive. The current study is to investigate the role of the bone marrow-derived mesenchymal stem cells (BM-MSCs) lncRNA (Neat-1 and Hotair1) and miRNA (mir-21-5p, mir-144-5p, and mir-664-5p) in mitigating ovarian granulosa cell apoptosis as well as searching BM-MSCs in altering the expression of ovarian and hypothalamic IGF-1 – kisspeptin system in connection to HPG axis in a cyclophosphamide-induced ovarian failure rat model. Sixty mature female Sprague Dawley rats were divided into 3 equal groups; control group, premature ovarian insufficiency (POI) group, and POI + BM-MSCs. POI female rat model was established with cyclophosphamide. The result revealed that BM-MSCs and their conditioned media displayed a significant expression level of Neat-1, Hotair-1, mir-21-5p, mir-144-5p, and mir-664-5p. Moreover, BM-MSCs transplantation in POI rats improves; the ovarian and hypothalamic IGF-1 – kisspeptin, HPG axis, ovarian granulosa cell apoptosis, steroidogenesis, angiogenesis, energy balance, and oxidative stress. BM-MSCs expressed higher levels of antiapoptotic lncRNAs and microRNAs that mitigate ovarian insufficiency.

*Correspondence:
Iulia Maria Bucur
Iulia.bucur@usvt.ro
Ahmed Hamed Arisha
vetahmedhamed@zu.edu.eg
Tarek Khamis
t.khamis@vet.zu.edu.eg

Full list of author information is available at the end of the article

Keywords lncRNA, microRNAs, Premature ovarian failure, Cyclophosphamide, BM-MSCs, HPG

Introduction

Female infertility is the inability to conceive a pregnancy for one year. Due to its significant impact on a substantial worldwide population, infertility has garnered considerable attention. The primary focus of clinical research has been the advancement of novel therapeutic interventions aimed at preventing and managing infertility and improving the overall quality of life for affected patients [1]. One of the significant factors contributing to infertility and abnormal ovarian function is ovulatory dysfunction. POI and polycystic ovary syndrome (PCOS) are the two main conditions that cause ovarian dysfunction and are linked to infertility [2]. Primary ovarian insufficiency, often POI, is a complex and mysterious medical condition. According to statistical data, the prevalence of POI is estimated to be approximately 1 in 250 women under the age of 35 and 1 in 100 women under 40 years old. Yoon SY [3] POI is characterized by oligomenorrhea or amenorrhea, increased follicle-stimulating hormone (FSH), and low estradiol levels [4].

The complex interaction of many regulatory signals within the hypothalamic-pituitary-ovarian (HPO) axis is crucial for developing and maintaining female reproductive potential. The intricate neurohormonal system controls ovarian hormone secretion and the intermittent release of oocytes during ovulation [5]. Recently, stem cell therapy has gained acceptance as a prospective and alternative therapeutic approach, allowing the repair and restoration of the normal function of injured tissues [6, 7]. Interestingly, Mesenchymal stromal cells (MSCs) are a subset of adult stem cells derived from the mesoderm, a germ layer in embryonic development. These cells can undergo self-renewal and differentiate into many cell types derived from both ectoderm and endoderm, as well as mesoderm lineages, including osteocytes, chondrocytes, and adipocytes. MSCs are ubiquitously present in nearly all types of tissues. Mesenchymal stem cells can be readily obtained from various sources, including bone marrow, fetal liver, muscle, lung, adipose tissue, and the umbilical cord [8]. For ovarian dysfunction, MSCs can migrate directly and impulsively to the damaged ovary and survive there while being stimulated by multiple factors that facilitate ovarian recovery [9–11].

In "next generation" biology, non-coding RNA (ncRNA) is thought to be the research area of interest. Yet, its intricate interaction with POI remains elusive. Single-stranded RNAs with more than 200 nucleotides (nt) are referred to as long non-coding RNAs (lncRNAs), and they have a role in many disorders [12]. It is well-known that the incidence and progression of POI are closely correlated with the aberrant transcription of cellular lncRNA [13]. For instance, lncRNA DLEU1 accelerated the apoptosis of OGCs and was significantly elevated in POI ovarian tissues compared to the control [14]. Additionally, it has been previously noted that lncRNA HOTAIR overexpression decreased hamster ovary cell apoptosis [15]. According to numerous reports, nuclear enriched abundant transcript 1 (NEAT1), a lncRNA, was thought to act as an oncogene in ovarian cancer and other human malignancies by preventing cancer cells from dying off (apoptosis) [16, 17]. Although the relationship between NEAT1 and Hotair-1 in the progress of POI has been hypothesized, the precise mechanism is yet unknown. Short non-coding RNA (sncRNAs) called microRNAs (miRNAs), which have a length of around 22 nt, are primarily in control of post-transcriptionally regulating gene expression [18]. According to reports, POI progresses as a result of miRNAs being improperly regulated [19, 20]. Yang et al. discovered that miR-144-5p was beneficial in preventing POI caused by cyclophosphamide intraperitoneally (CTX) [19]. The long non-coding RNA (Hotair-1) acts Through a NOTCH1-mediated mechanism, as a microRNA-34a-5p sponge to decrease nucleus pulposus cell death [21]. Moreover, through the sponging of miR-125a-5p by the long non-coding RNA NEAT1, cardiomyocyte apoptosis is suppressed [22].

Multiple studies have indicated that the secretome of mesenchymal stem cells (MSCs) plays a crucial role in the therapeutic impact on reproduction. This is attributed to the secretome's abundance of bioactive molecules that effectively promote and sustain ovarian functions. The molecules under consideration encompass IGF, VEGF, and other growth factors that elicit cellular development, differentiation, and immunoregulation, thus facilitating the restoration of ovarian functions [23]. Recently, there has been a prevailing agreement that the paracrine action of mesenchymal stem cells (MSCs) holds more significance compared to their differentiation capacity. The regenerative properties of transplanted MSCs can be ascribed to pathways encompassing both direct cell-cell interaction and the release of bioactive chemicals that facilitate angiogenesis and tissue regeneration. As a result, the scarring process is suppressed, the immune and inflammatory reactions are regulated, and the activation of tissue-specific progenitor cells occurs [9].

Interestingly, MSCs' secretome comprised lncRNAs which play a vital role in their paracrine regenerative mechanism such a role activating the internal repairing mechanism via initiating resident quiescent tissue stem cells and suppressing several pro-apoptotic microRNAs [24, 25]. Furthermore, MSCs' secretomes expressed several microRNAs such as mir-21 [26], mir-144-5p [19],

and mir-664-5p [27] which suppress ovarian granulosa cell apoptosis. However, the exact mechanism of ovarianRNA; mir-21-5p, mir-144-5p, and mir-664-5p, also their lncRNA Neat-1, and Hotair-1 and their miRNA and mRNA targets in the modeling of the ovarian insufficiency remain elusive. Thus, the present study was designed to explore the role of the BM-MSCs lncRNA (Neat-1 and Hotair1) and miRNA (mir-21-5p, mir-144-5p, and mir-664-5p) in mitigating ovarian granulosa cell apoptosis as well as searching BM-MSCs in altering the expression of ovarian and hypothalamic IGF-1 – kisspeptin system in connection to HPG axis in cyclophosphamide-induced ovarian failure rat model.

Materials and methods

Animals

A total of sixty Sprague-Dawley rats, classified as healthy adult females weighing 150 to 200 g and aged 6 to 8 weeks, were procured from the animal facility located at the Faculty of Veterinary Medicine, Zagazig University, Egypt. The rats in the study were provided with appropriate and ethical care, and the research procedures were authorized by the Institutional Animal Care and Use Committee of Badr University in Cairo (Reference No. BUC-IACUC/VET/134/A/2023).

Chemicals

The Cyclophosphamide utilized in this study was procured from (Baxter, USA). The DMEM medium, streptomycin, penicillin, phosphate-buffered saline (PBS), and fetal bovine serum (FBS) were acquired from Lonza Bioscience. Qiazol was supplied from (Qiagen, Germany), chloroform HPLC grade, isopropanol HPLC grade, Ethanol HPLC grade (Sigma, Aldrich), high-capacity reverse transcriptase cDNA kit (Applied Biosystem Massachusetts, USA), TopReal Sybergreen master mix (Enzynomics, Korea). ELISA kit for serum hormonal assays of FSH, LH, PRL, and E2 was supplied by (Cusabio, China). Antibodies for immunohistochemistry were bought from (primary and secondary) for VEGF, and Kiss-1 was obtained from (Abcam), rat fibroblast cell line obtained from the laboratory of stem cells and regenerative medicine research faculty of veterinary medicine, Zagazig University, Egypt.

Isolation and culturing of BM-MSCs

According to the protocol of Smajilagić A, Aljičević M, Redžić A, Filipović S and Lagumdžija A [28] 12 weeks old rats were sacrificed, and their femur and tibia were aseptically extracted. The cancellous bone was extracted from the femur and tibia specimens and subjected to 3–5 washes using 1x phosphate-buffered saline (PBS) obtained from Lonza Bioscience. Subsequently, the bone marrows were rinsed using Dulbecco's Modified Eagle Medium (D-MEM) culture media (Lonza, Bioscience) containing 10% (V/V) FBS (Lonza, Bioscience) and 50 IU L-1 penicillin, 2mM L-glutamine, 50 µg mL-1 streptomycin (Lonza, Bioscience). The released cells were collected and placed in a culture flask with a surface area of 75 cm^2. The flask contained 15 ml of D-MEM culture media from Lonza Bioscience. The cell cultures were incubated at 37° C in a controlled environment with a humidity level of 95% air and 5% carbon dioxide. The cells were left to adhere for three days. Following this, the non-adherent cell population was eliminated, and the culture medium was substituted with fresh culture D-MEM. The culture media underwent biweekly changes. Following the initial passage, the adhering cells were dissociated using a solution of 0.25% trypsin-EDTA (Lonza, Bioscience) and subsequently cultivated for three consecutive passages.

As observed using an inverted microscope, MSCs in culture were identified based on their ability to adhere to the culture surface and their distinct morphological features, including fusiform, circular, and spindle forms. The cells obtained from the third passage were subjected to flow cytometry analysis to assess the presence of specific surface markers associated with mesenchymal stem cells, they were negative for (CD45, CD34, and HLA-DR) and positive for (CD90, CD73, and CD105). To trace the homing of the transplanted BM-MSCs in the ovarian tissues, the BM-MSCs were trypsinized with 0.25% trypsin EDTA, washed twice with PBS then labeled with red fluorescent vital cell linker stain PKH26 (Sigma Aldrich, USA; PKH26GL)) following the supplier guidelines. Furthermore, long-coding RNAs (Hotair1 and Neat-1) and miRNA (mir-21-5p, mir-664-5p, and mir-144-5p) expression were detected in BM-MSCs and BM-MSCs conditioned media that were compared to the expression level in the rat fibroblast cell line obtained from the laboratory of stem cells and regenerative medicine research faculty of veterinary medicine, Zagazig University, Egypt.

Experimental design

A total of sixty mature female Sprague Dawley rats were randomly allocated into three equal groups. A total of 20 rats were assigned to each group; G1: Control group, the rats were injected IP with 0.25 mL with PBS daily for 14 consecutive days; G2: POI (Premature ovarian insufficiency),. G3: POI+BM-MSCs (premature ovarian failure+bone marrow mesenchymal stem cells); after successful induction of the POI, the rats were transplanted with BM-MSCs one IP injection at a dose of 2×10^7 suspended in 0.25 mL of PBS. POI was induced in female rats with Intraperitoneal (IP) cyclophosphamide (50 mg/kg) followed by IP daily cyclophosphamide injection of (8 mg/kg) for 14 consecutive days [29]. BM-MSCs were transplanted intraperitoneally at a dose of (2×10^7) cells for each rat.

Blood and tissue sample collection

After 12 weeks from the initial cyclophosphamide dosing, blood samples were obtained from the retro-orbital venous plexus, and the serum was afterward separated and preserved at a temperature of -20ºC for the enzyme-linked immunosorbent assay (ELISA) and biochemical analysis. The hypothalamus, pituitary, and ovaries were collected and preserved in 1 ml of Qiazol (Qiagen, Germany) at a temperature of -80ºC. These samples will be utilized for RNA extraction and subsequent gene expression analyses. A total of eight ovaries from each experimental group were obtained and preserved in a 10% neutral formalin buffer solution for further histopathological and immunohistochemical analyses. Ten right ovaries of different experimental groups were homogenized separately with potassium chloride buffer solution 1.15% for obtaining 10% ovarian tissue homogenate 1/10 (w/v). The homogenate was centrifuged for 15 min at 4000 rpm and stored at -80ºC for further oxidant/antioxidant activity use.

Assay of the serum hormonal level and ovarian oxidative stress markers

Serum levels of the estrogen (E2), follicle–stimulating hormone (FSH), Prolactin (PRL), and Luteinizing hormone (LH) were measured using sandwich ELISA kits (Cusabio, China) according to manufacture instructions and following the method used in Al-Shahat A, Hulail MAE, Soliman NMM, Khamis T, Fericean LM, Arisha AH and Moawad RS [30]. The serum level of the anti-mullerian hormone (AMH) was measured using sandwich ELISA kit (MyBioSource, USA, #MBS453381) according to the provider's instructions. Moreover, the ovarian tissue homogenates of the different experimental groups were used for assaying the oxidative stress markers, Malonaldehyde (MDA), Superoxide dismutase (SOD), reduced Glutathione (GSH), Catalase (CAT), and Total antioxidant capacity (TAC) using kits supplied by Diagnostic and Research Reagents (Giza, Egypt).

Real-time PCR analysis

The total RNA of the BM-MSCs, BM-MSCs conditioned media, rat fibroblast cells, and pituitary, hypothalamus, and ovarian tissue of the different experimental groups' was extracted using Qiazol (Qiagen, Germany). RNA purity and concentration were assessed using the NanoDrop® ND-1000 Spectrophotometer (NanoDrop Technologies, Wilmington, Delaware, USA). From the total extracted RNA, 500 ng was used for cDNA synthesis using a high-capacity reverse transcriptase kit (Applied Biosystem, Foster City, CS, USA) following the supplier's instructions. Moreover, cDNA for the microRNAs (U6, mir-34a, mir-125a, mir-21-5p, mir-664-5p, and mir-144-5p) of the ovarian tissue, BM-MSCs, BM-MSCs conditioned media, and rat fibroblast cells were synthesized with specific stem-loop primer for each microRNA mentioned in Table 1 using miScript II reverse transcription kit (Qiagen, Valencia, CA) following the supplier instruction. The mRNA target for the microRNA were defined using TargetScan online software https://www.targetscan.org/vert_80/, on the other hand, the mature sequence for each miRNAs were got form microRNAs online data base https://www.mirbase.org/, and the stem-loop, forward, and reverse primer of each miRNA were designed using online stem-loop primer designing tool http://www.srnaprimerdb.com/.

The detection of the integration of male BM-MSCs into female ovarian tissues was accomplished by assessing the relative mRNA expression of the sex determination region on the male Y chromosome (SRY gene) in the ovarian tissues of the female rat recipient [31]. The gene expression analysis for ovarian, BM-MSCs, BM-MSCs conditioned media, and rat fibroblast cells miRNA (U6, mir-34a, mir-125a, mir-21-5p, mir-664-5p, and mir-144-5p), long-noncoding RNA (Neat-1 and Hotair1), ovarian, hypothalamic, and pituitary mRNA expression for (Notch-1, P53, Casp-3, BCL-2, Gapdh, Sry, IGF-1, Kiss-1, Kiss1r, GnRH, GnRhr, GnIH, FSH-1β, LH-1β, GLP-1, PPAR-α, StAR, CYP-17A1, CYP-11A1, CYP-19A1, HSD-17β3) were assayed using RotorGene Q 2 plex real-time PCR system (Qiagen, Germany) with a primer sequence synthesized by (Sangon Biotech, Beijing, China) and listed in Table 1. The relative gene expression was determined via the $2^{-\Delta\Delta CT}$ method, according to Livak KJ and Schmittgen TD [32], with Gapdh serving as the reference gene for mRNA and long-noncoding RNA as well as U6 for normalizing data of the miRNA expression.

Histological and immunohistochemical analysis

The ovarian tissue of the different experimental groups was fixed in neutral formalin buffer 10% overnight, then serially passaged in graded ethanol concentration for tissue dehydration, then submerged for 20 min in benzene, and fixed in paraffin wax blocks. The tissue paraffin wax blocks were sectioned into 5-micron sections. After that, the sections were deparaffinized with xylene and stained with H&E for histological examination by light microscope [33]. Immunohistochemistry for VEGF and Kiss-1 was done using a primary polyclonal rabbit anti-VEGF-A (ABclonal, Cat. No. # A0280) and a primary rabbit polyclonal anti-kisspeptin antibody (Bioss, Cat. No. # bs-0749R) and their related secondary antibodies. Antigens were retrieved via boiling for 15 min in citrate buffer pH 6, followed by blocking the endogenous peroxidase activity with hydrogen peroxide 3% for 20 min. For blocking the nonspecific antigen, goat serum was used and incubated at 37 ºC for 30 min. The sections were incubated

Table 1 PCR primer and stem-loop primers for microRNA sequences

Gene	Forward primer (5′–3′)	Reverse primer (5′–3′)	Accession No	Product size
Kiss-1	TGCTGCTTCTCCTCTGTGTGG	ATTAACGAGTTCCTGGGGTCC	NM_181692.1	110
Kiss-1r	CTTTCCTTCTGTGCTGCGTA	CCTGCTGGATGTAGTTGACG	NM_023992.1	102
GnRH1	AGGAGCTCTGGAACGTCTGAT	AGCGTCAATGTCACACTCGG	NM_012767.2	100
GnRHr	TCAGGACCCACGCAAACTAC	CTGGCTCTGACACCCTGTTT	NM_031038.3	182
GnIH	AGAGCAACCTAGGAAACGGGTGTT	AGGACTGGCTGGAGGTTTCCTATT	NM_023952.1	84
Star	CCCAAATGTCAAGGAAATCA	AGGCATCTCCCCAAAGTG	NM_031558.3	187
CYP11A1	AAGTATCCGTGATGTGGG	TCATACAGTGTCGCCTTTTCT	NM_017286.3	127
CYP17A1	TGGCTTTCCTGGTGCACAATC	TGAAAGTTGGTGTTCGGCTGAAG	NM_012753.2	90
CYP19A1	GCTGAGAGACGTGGAGACCTG	CTCTGTCACCAACAACAGTGTGG	NM_017085.2	178
SRY	CTAGAGCTGCACACCAGTCC	Tgggtatccagtggggatgt	NM_001409365.1	77
IGF-1	AAGCCTACAAAGTCAGCTCG	GGTCTTGTTTCCTGCACTTC	NM_001082477.2	166
GLP-1	CACCTCCTCTCAGCTCAGTC	CGTTCTCCTCCGTGTCTTGA	NM_012707.2	128
PPAR-α	GTCCTCTGGTTGTCCCCTTG	GTCAGTTCACAGGGAAGGCA	NM_013196.2	176
PDCD4	CGGCCCGAGGGGATTCTAAA	GGGTCAGTGGGGTTCACATT	NM_022265.3	123
PTEN	ATACCAGGACCAGAGGAAACC	TTGTCATTATCCGCACGCTC	NM_031606.2	101
notch-1	CCTTGCTCTGCCTAACGCT	ATTCAGGCAGGTCCCACTTG	NM_001105721.1	80
p53	CCCCTGAAGACTGGATAACTGT	TCTCCTGACTCAGAGGGAGC	NM_030989.3	75
BCL-2	GACTGAGTACCTGAACCGGCATC	CTGAGCAGCGTCTTCAGAGACA	NM_016993.1	135
Hotair-1	CCTTATAAGCTCATCGGAGCA	CATTTCTGGGTGGTTCCTTT	XR_005503470.1	
NEAT-1	AAGGCACGAGTTAGCCGCAAAT	TGTGCACAGTCAGACCTGTCATTC	XR_005494740.1	
mir-34a	AACACGCTGGCAGTGTCTTA	GTCGTATCCAGTGCAGGGT		
mir-21	AAGCGACCTAGCTTATCAGACT	GTCGTATCCAGTGCAGGGT		
mir-125a	AACAAGTCCCTGAGACCCTTTA	GTCGTATCCAGTGCAGGGT		
mir-664-5p	AACAAGCTGGCTGGGGAAA	GTCGTATCCAGTGCAGGGT		
mir-144-5p	AGCCAGCGGGATATCATCATATA	GTCGTATCCAGTGCAGGGT		
U6	GCTCGCTTCGGCAGCACA	GAGGTATTCGCACCAGAGGA		
Stem-loop primers for microRNA				
mir34a	GTCGTATCCAGTGCAGGGTCCGAGGTATTCGCACTGGATACGACACAACC			
mir125a	GTCGTATCCAGTGCAGGGTCCGAGGTATTCGCACTGGATACGACTCACAG			
mir-664	GTCGTATCCAGTGCAGGGTCCGAGGTATTCGCACTGGATACGACCCAATC			
mir-144-5p	GTCGTATCCAGTGCAGGGTCCGAGGTATTCGCACTGGATACGACACTTAC			
mir-21-5p	GTCGTATCCAGTGCAGGGTCCGAGGTATTCGCACTGGATACGACTCAACA			

with the primary rabbit polyclonal anti-VEGF-A (dilution rate, 1:200) and anti-Kiss-1 (dilution rate, 1:200) antibody overnight at 4 ºC then were subjected to incubation with the secondary antibody and subsequently stained with DAB. For quantifying positive immunoreaction, three slides for each rat and ten fields for each slide were evaluated for the immunostaining density of VEGF-A and Kiss-1 and determined by using FIJI/ImagJ® software [34].

Statistical analysis

The statistical analysis was performed using GraphPad Prism Version 9.2 software, (GraphPad Software Inc. in San Diego, California, USA). The data is presented in the form of the mean ± standard error of the mean (SEM). The statistical analysis consisted of performing a one-way analysis of variance (ANOVA) test, followed by a post hoc Tukey test to facilitate pairwise comparisons. The results exhibited statistical significance, as shown by a p-value below 0.05.

Results

Bm-MSCs identification and homing

The present study's findings indicate that the isolated cells adhered to the culture flask surface, displaying a round morphology on the third day of culture and transitioning to a spindle form by the seventh day of culture (Fig. 1A & B). Moreover, the isolated cells were positive for CD105, CD90, and CD73, however, showed negative reaction with CD45, CD34, HLA-DR (Fig. 1C – I). Interestingly, the tracking of the transplanted BM-MSCs revealed that BM-MSCs could be homed to the injured ovarian tissue in the POI + BM-MSCs group which was validated by the positive red florescent color of PKH-26 stained BM-MSCs during examination of the ovarian tissue under florescent microscope and confirmed with the mRNA expression of SRY gene compared to a positive control for SRY expression (rat testicular tissue) (Fig. 1K & L).

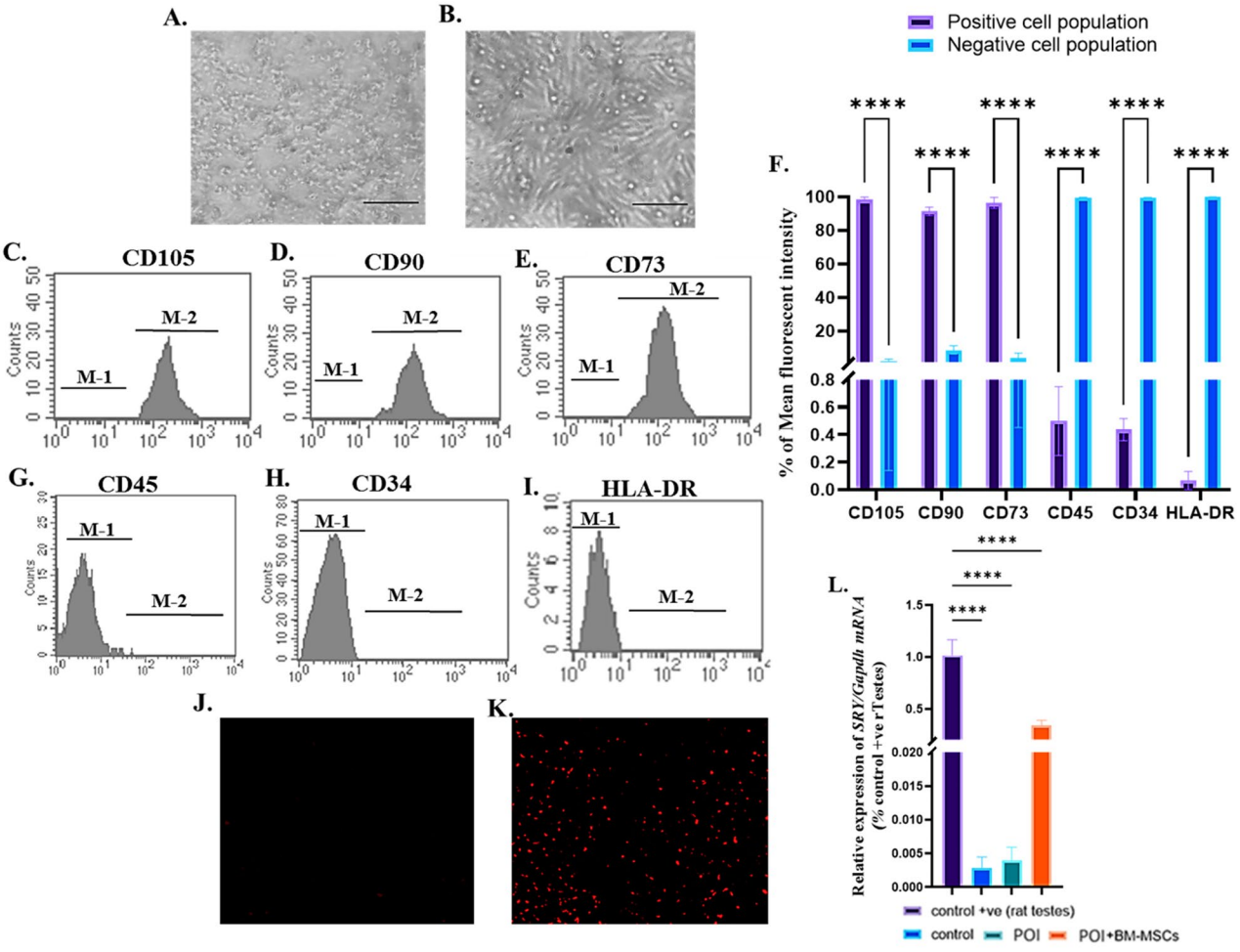

Fig. 1 BM-MSCs identification and homing (**A** – **L**). **A**. a representative photomicrograph of BM-MSCs on the 3rd of culture showed, **B**. a representative photomicrograph of BM-MSCs on the 7th day of culture, **C**. flow cytometry analysis of CD105, **D**. flow cytometry analysis of CD90, **E**. flow cytometry analysis of CD73, **F**. % of mean fluorescent intensity of positive cell population for (CD105, CD90, CD73, CD45, CD34, and HLA-DR), **G**. flow cytometry analysis of CD45, **H**. flow cytometry analysis of CD34, **I**. flow cytometry analysis of HLA-DR, **J**. a reprehensive photomicrograph of control group under the fluorescent microscope showing negative fluorescent signal, Scale bar 100 µm, **K**. a reprehensive photomicrograph of POI + BM-MSCs group ovarian tissue under fluorescent microscope showing positive red fluorescent signal of PKH-26 stained BM-MSCs, Scale bar 100 µm, and **L**. Relative expression of SRY/Gapdh mRNA of the different treated group compared to rat testicular tissue for ensuring BM-MSCs homing

Expression of anti-apoptotic long non-coding RNA (Neat-1 & Hotair-1) of BM-MSCs and their conditioned media

The result of the present study revealed that the expression of the anti-apoptotic long non-coding RNA Hotair-1 and Neat-1 were detected with a marked significant level in both BM-MSCs ($p<0.0001$) and their conditioned media ($p<0.01$) compared with the rat fibroblast cells as a control (Fig. 2A).

Effect of BM-MSCs transplantation on the ovarian expression of anti-apoptotic LncRNA and their miRNA and mRNA targets

The outcomes of the current investigation showed that the POI group displayed a significant ($p<0.0001$) downregulation in the relative expression of the anti-apoptotic; lncRNA (Neat-1 & Hotair-1) and mRNA (BCL-2 & Notch-1) with significant upregulation in the expression of the pro-apoptotic miRNA (mir-34a & mir-125a) (Fig. 2B – G). Surprisingly, BM-MSCs transplantation in the POI female rats significantly ($p<0.0001$) upregulated the expression of Neat-1, Hotair-1, BCL-2, and Notch-1 as well as downregulated the expression of mir-34a and mir-125a compared with POI group (Fig. 2B – G). Moreover, there was a significant ($p<0.05$) downregulation in the relative expression of Neat-1, Hotair-1, BCL-2, and Notch-1, with a significant ($p<0.01$) upregulation in mir-34a and mir-125a expression in the POI + BM-MSCs group than the control group (Fig. 2B – G).

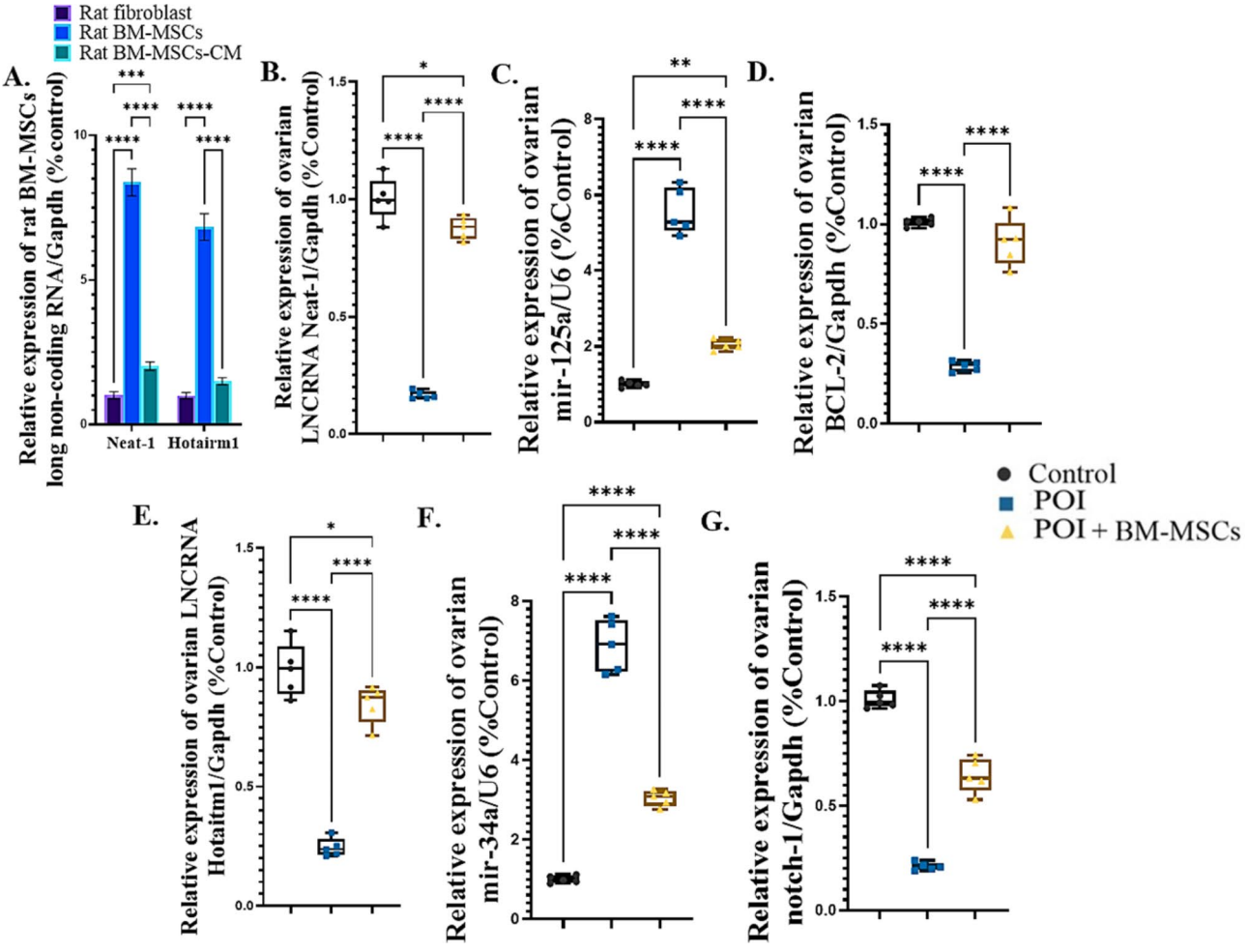

Fig. 2 Expression of anti-apoptotic long non-coding RNA (Neat-1 & Hotair-1) of BM-MSCs and their conditioned media and Effect of BM-MSCs transplantation on the ovarian expression of anti-apoptotic LncRNA and their miRNA and mRNA targets (**A – G**). **A**. Expression of anti-apoptotic long non-coding RNA (Neat-1 & Hotair-1) in BM-MSCs and BM-MSCs conditioned media in comparison with rat fibroblast cells as a control, **B**. Relative expression of ovarian lncRNA Neat-1/Gapdh, **C**. relative expression of ovarian mir-125a/U6, **D**. Relative expression of ovarian BCL-2/Gapdh, **E**. Relative expression of lncRNA Hotair-1/Gapdh, **F**. Relative expression of ovarian mir-34a/U6, and **G**. Relative expression of ovarian Notch-1/Gapdh

Expression of anti-apoptotic miRNAs (mir-21, mir-664, mir-144) of BM-MSCs and their conditioned media

The findings of the contemporary work illustrated that the expression level of the anti-apoptotic miRNAs; mir-21-5p, mir-664-5p, and mir-144-5p were found to be significantly ($p<0.0001$) upregulated in BM-MSCs and their conditioned media than the rat fibroblast cells (Fig. 3A).

Effect of BM-MSCs transplantation on the ovarian expression of anti-apoptotic miRNAs and their target genes

The result of the present investigation showed that the anti-apoptotic miRNAs mir-21-5p, mir-664-5p, and mir-144-5p were significantly ($p<0.0001$) downregulated, however, the pro-apoptotic markers P53 and caspase-3 were significantly upregulated in the POI groups than the control one (Fig. 3B – F). On the contrary, POI group treated with BM-MSCs elucidated a significant ($p<0.0001$) upregulation in the expression of anti-apoptotic miRNAs; miRNAs mir-21-5p, mir-664-5p, mir-144-5p, and downregulation in the expression of pro-apoptotic markers P53 and caspase-3 compared with the POI groups (Fig. 3B – F). Moreover, POI+BM-MSCs cells showed a significant ($p<0.001$); downregulation in the expression of mir-21-5p, mir-664-5p, mir-144-5p and upregulation in the P53 and caspase-3 expression than the control group (Fig. 3B – F).

Effect of BM-MSCs transplantation on mRNA expression of IGF-1/HPG axis of the POI rats

The results of the present study showed a significant ($p < 0.0001$) downregulation in the relative mRNA expression of the hypothalamic IGF-1, Kiss-1, Kiss-1r, GnRH, and pituitary GnRhr in the POI group compared to the control one (Fig. 4A – F). However, hypothalamic GnIH of the POI rats was significantly ($p < 0.0001$) upregulated

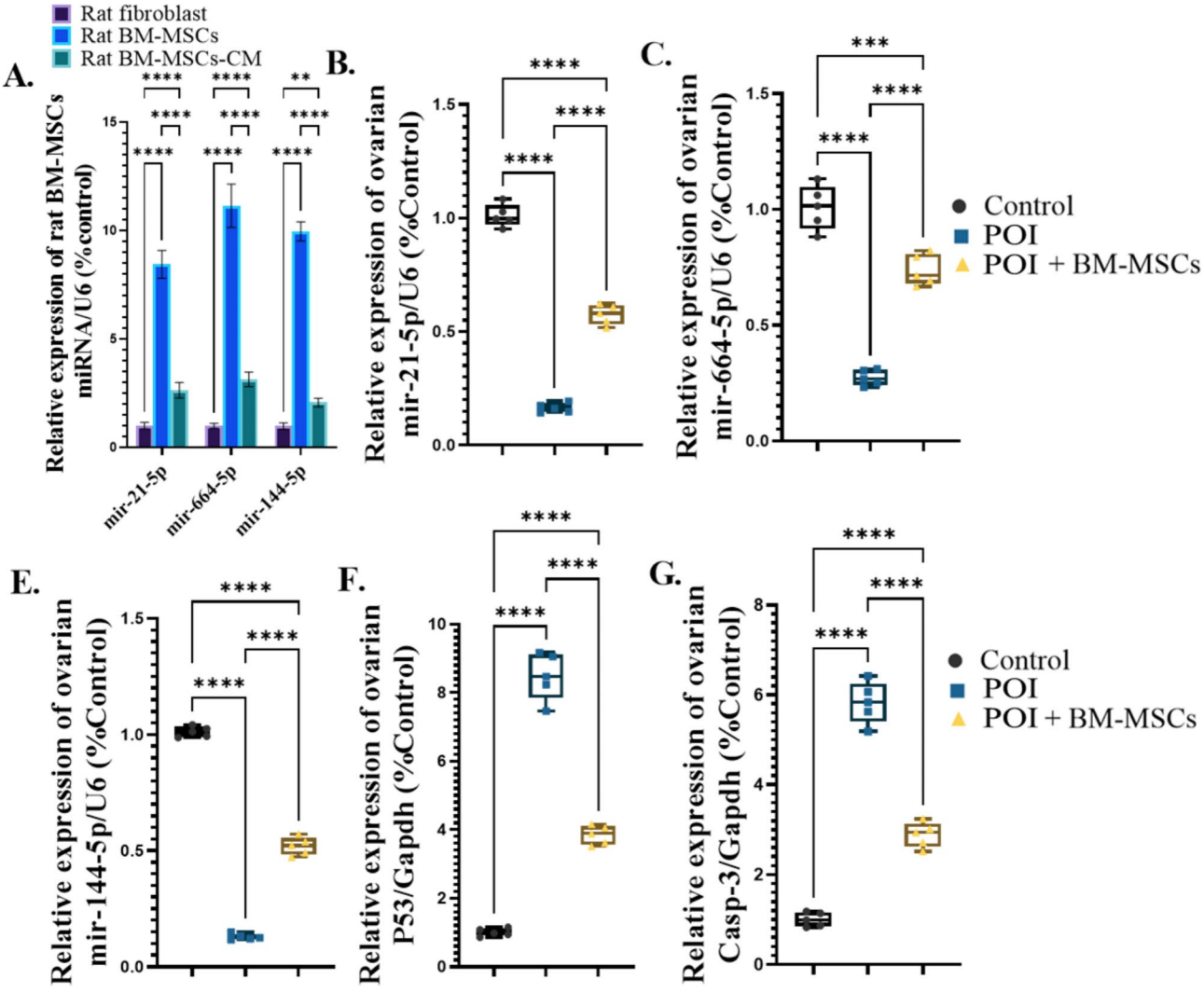

Fig. 3 Expression of anti-apoptotic miRNAs (mir-21, mir-664, mir-144) of BM-MSCs and their conditioned media and Effect of BM-MSCs transplantation on the ovarian expression of anti-apoptotic miRNAs and their target genes (**A – F**). **A**. Relative expression of anti-apoptotic miRNAs; mir-21-5p, mir-664-5p, mir-144-5p in BM-MSCs and their conditioned media compared to rat fibroblast cells as a control, **B**. relative expression of ovarian mir-21-5p/U6, **C**. relative expression of ovarian mir-664-5p/U6, **D**. Relative expression of ovarian mir-144-5p/U6, **E**. Relative expression of ovarian P53/Gapdh, and **F**. Relative expression of ovarian caspase-3/Gapdh

in comparison to control rats (Fig. 4D). On the other hand, BM-MSCs transplantation induced a significant ($p < 0.0001$) improvement in the relative expression of hypothalamic IGF-1, Kiss-1, Kiss-1r, GnRH, GnIH, and pituitary GnRhr compared with the POI group (Fig. 4A – F). On the contrary, BM-MSCs + POI group elicited a significant downregulation of the relative mRNA expression of IGF-1 ($p < 0.01$), Kiss-1 ($p < 0.05$), Kiss-1r, GnRH, and pituitary GnRhr ($p < 0.0001$) and significant ($p < 0.0001$) upregulation in the relative mRNA expression of hypothalamic GnIH compared to the control group (Fig. 4A – F.).

Effect of BM-MSCs transplantation on the hormonal levels of the POI rats

The serum levels of (FSH, LH, and E2) were significantly decreased ($p < 0.001$), and relative mRNA expression of the pituitary (FSH-1β and LH-1β) were significantly downregulated ($p < 0.0001$) in the POI group than the control one (Fig. 5A – F). However, the serum level of Prolactin and AMH were significantly increased ($p < 0.001$) in the POI group than the control one (Fig. 5F). In contrast, the findings of the current investigation demonstrated a statistically significant rise ($p < 0.001$) in the serum concentrations of (FSH, LH, and E2) and a significant upregulation ($p < 0.0001$) in the relative mRNA expression of the pituitary (FSH-1β and LH-1β) in the POI + BM-MSCs group compared to the POI group

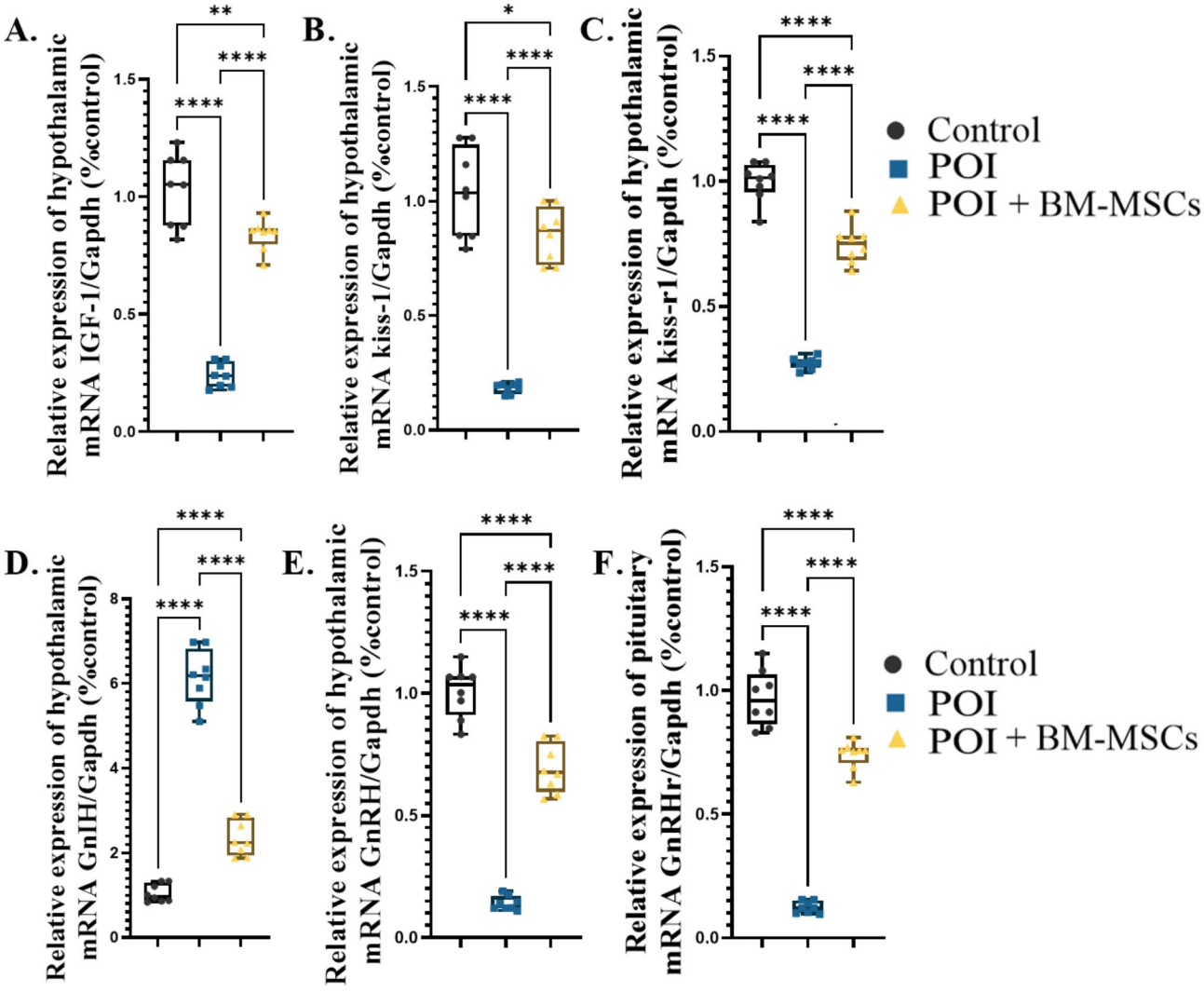

Fig. 4 Effect of BM-MSCs transplantation on mRNA expression of IGF-1/HPG axis of the POI rats (**A** – **F**). **A**. hypothalamic mRNA IGF-1, **B**. hypothalamic mRNA Kiss-1, **C**. hypothalamic mRNA Kiss-r1, **D**. hypothalamic mRNA GnIH-1, **E**. hypothalamic mRNA GnRH, and **F**. hypothalamic mRNA GnRHr. The values represent the average of 6 to 8 rats in each group ± SEM *$p < 0.05$, **$p < 0.01$, ****$p < 0.0001$

(Fig. 5A – F). Meanwhile, the serum level of Prolactin and AMH were significantly decreased (p ˂ 0.0001) in the POI+BM-MSCs group than the POI group (Fig. 5F). However, POI+BM-MSCs groups provoked a significant (p ˂ 0.001) decrease in the serum levels of (FSH, LH, and E2), a significant (p ˂ 0.001) downregulation in the relative mRNA expression of pituitary LH-1β, and a significant (p ˂ 0.01) increase in the serum prolactin and AMH level than the control one (Fig. 5A – F).

Effect of BM-MSCs transplantation on the ovarian oxidative stress markers of the POI rats

The outcomes of the current investigation showed a significant ($p<0.0001$) increase in the lipid peroxidation marker MDA and a significant ($p<0.0001$) decrease in the activity of CAT, SOD, GSH, and TAC in the POI and POI+BM-MSCs groups compared to the control group (Fig. 6A – E). In contrast, the POI+BM-MSCs group elicited a significant ($p<0.0001$) decrease in the lipid peroxidation marker MDA and a significant increase in the activity of CAT, SOD, GSH, and TA compared to the POI group (Fig. 6A – E).

Effect of BM-MSCs transplantation on mRNA expression of ovarian IGF-1 – GLP-1 – PPAR-α / steroidogenesis pathway of the POI rats

The result of the present study illustrated a significant (p ˂0.0001) downregulation in the relative mRNA expression of the ovarian IGF-1, GLP-1, PPAR-α, StAR, CYP-11A1, CYP-19A1, and HSD-17β3 in the POI group compared to the control one (Fig. 7A – H). In contrast, The POI+BM-MSCs group showed a significant (p ˂0.0001) upregulation in the relative mRNA expression of the ovarian IGF-1, GLP-1, PPAR-α, StAR, CYP-11A1,

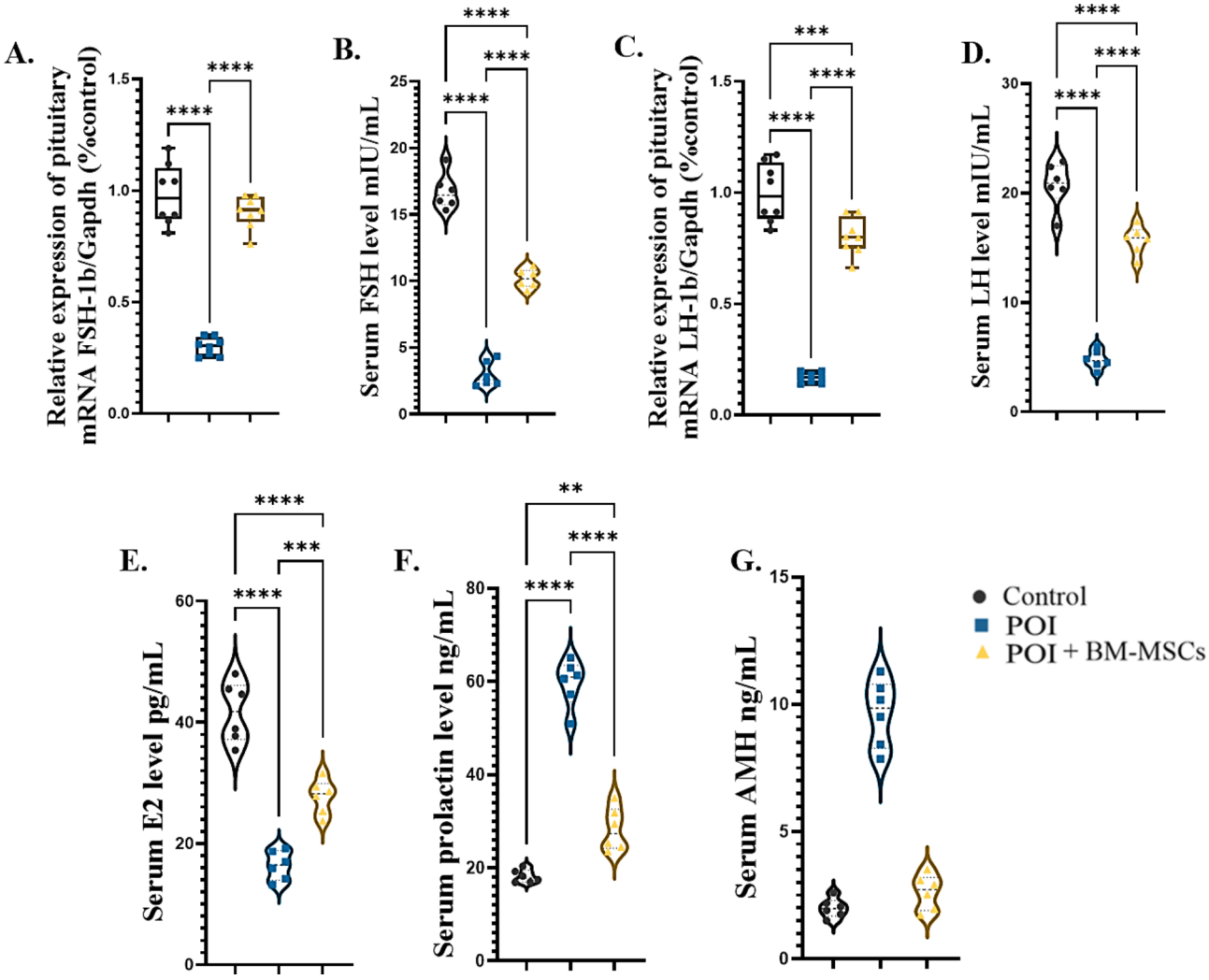

Fig. 5 Effect of BM-MSCs transplantation on the hormonal levels of the POI rats (**A** – **G**). **A**. Relative expression of pituitary mRNA FSH-1β, **B**. Serum FSH level mIU/mL, **C**. Relative expression of pituitary mRNA LH-1β, **D**. Serum LH level mIU/mL, **E**. Serum E2 level pg/mL, **F**. Serum prolactin level ng/mL, and **G**. Serum AMH level ng/mL. Values are the mean of 8 rats per group ± SEM *$p < 0.05$, **$p < 0.01$, ***$p < 0.001$, ****$p < 0.0001$

CYP-19A1, and HSD-17β3 than POI group (Fig. 5A – H). Meanwhile, BM-MSCs transplantation induced a significant downregulation in the relative mRNA expression of CYP-11A1 (p ˂0.0001), CYP-19A1 (p ˂0.01), and HSD-17β3 (p ˂0.05) than the control group (Fig. 7E – H).

Effect of BM-MSCs transplantation on the expression of ovarian kisspeptin system of the POI rats

Regarding the KiSS-1 immunostaining, the cytoplasmic immunoreactivities were detected in the germinal epithelium, interstitial stromal cells, and granulosa-lutein cells as intense, faint, and moderate expression in control, POI, and POI+BM-MSCs groups, respectively (Fig. 8A – F). The findings of the contemporary work showed a significant (p ˂0.0001) downregulation in the relative mRNA expression of ovarian Kiss-1, Kiss-r1, and protein expression of the ovarian Kiss-1 positive immunostaining in the POI group compared to the control one (Fig. 8A – I). Interestingly, The POI+BM-MSCs group showed a significant (p ˂0.0001) upregulation in the relative mRNA expression of ovarian Kiss-1, Kiss-r1, and protein expression of the ovarian Kiss-1 positive immunostaining compared to the POI group (Fig. 8A – I). However, BM-MSCs administration fails to bring the ovarian kisspeptin system to the normal physiological tone of the control group (Fig. 8A – I).

Effect of BM-MSCs transplantation on the expression of ovarian anti-angiogenic VEGF-A 165b isoform of the POI rats

The anti-angiogenic VEGFA isoform immunostaining was localized in the cytoplasm of the granulosa lutein cells. This immunoreactivity appeared faint, intense, and moderate in CON, POI, and POI+BM-MSCs groups,

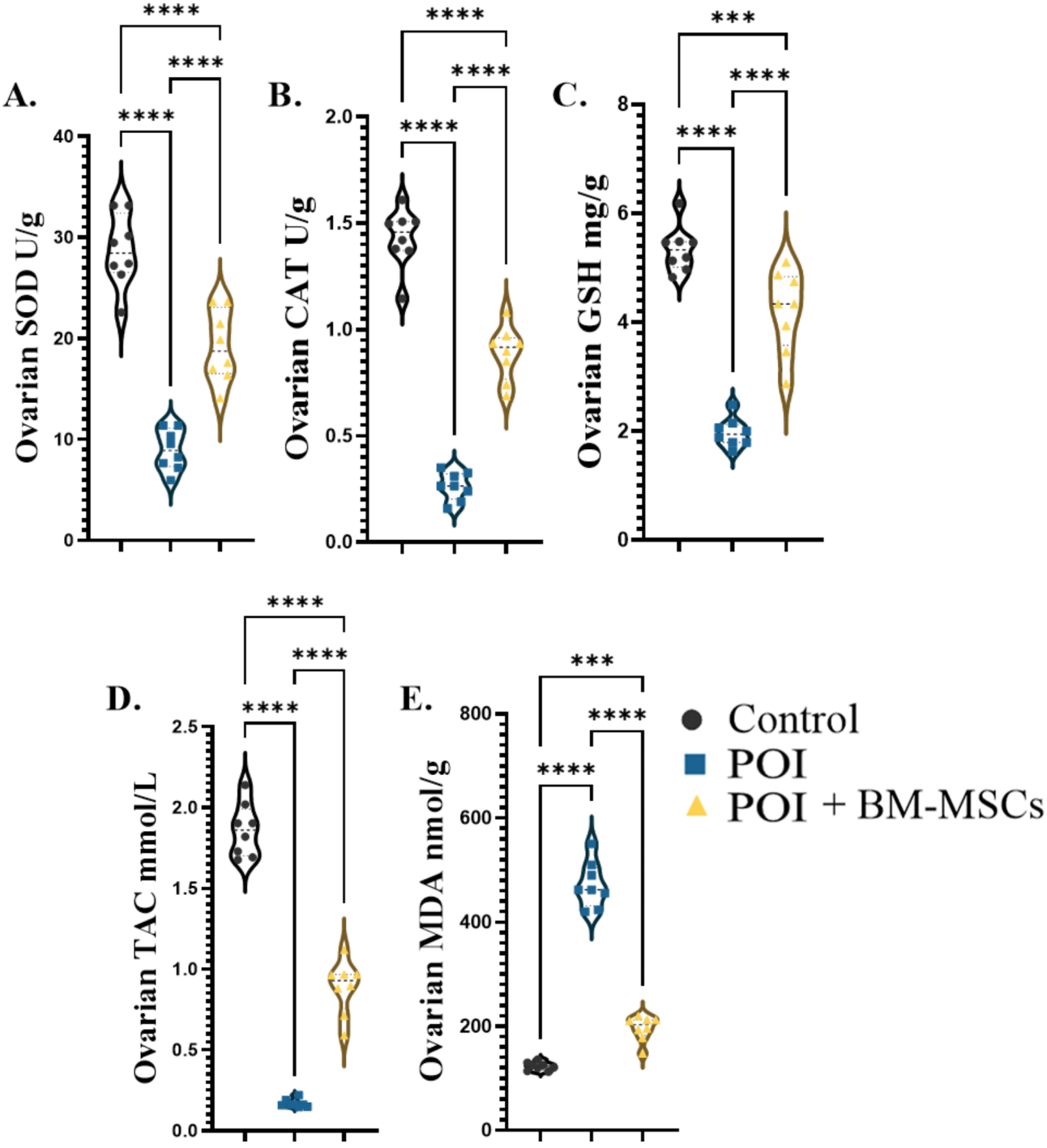

Fig. 6 Effect of BM-MSCs transplantation on the ovarian oxidative stress markers (**A** – **E**). **A**. SOD U/g, **B**. CAT U/g, **C**. GSH mg/g, **D**. TAC mmol/L, and **E**. MDA nmol/L. Values are the mean of 8 rats per group ± SEM ***$p < 0.001$, ****$p < 0.0001$

respectively (Fig. 9A – F). The result of the current study illustrated a significant ($p < 0.0001$) upregulation of the anti-angiogenic VEGF-A 165b isoform protein expression positive immunostaining of the POI group compared to control group (Fig. 9A – G). Surprisingly, BM-MSCs transplantation significantly ($p < 0.0001$) downregulated the expression of anti-angiogenic VEGF-A 165b isoform positive immunostaining than the POI group (Fig. 9A – G). But, BM-MSCs + POI group showed a significant ($p < 0.001$) upregulation in the expression of anti-angiogenic VEGF-A 165b isoform positive immunostaining compared to the control group (Fig. 9A – G).

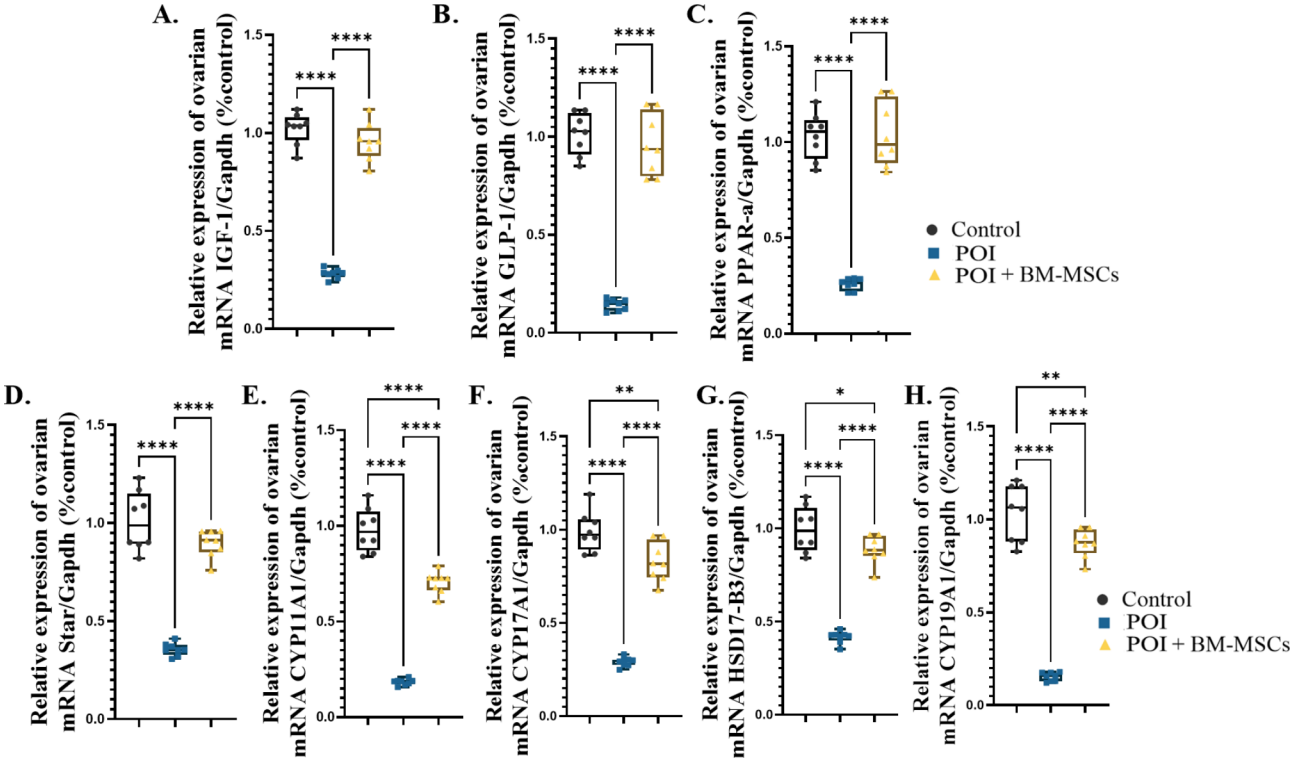

Fig. 7 Effect of BM-MSCs transplantation on mRNA expression of ovarian IGF-1 – GLP-1 – PPAR-α / steroidogenesis pathway of the POI rats (**A** – **H**). **A**. ovarian mRNA IGF-1, **B**. ovarian mRNA GLP-1, **C**. ovarian mRNA PPAR-α, **D**. ovarian mRNA StAR, **E**. ovarian mRNA CYP11A1, **F**. ovarian mRNA CYP17A1, **G**. ovarian mRNA HSD17B3, and **H**. ovarian mRNA CYP19A1. The values represent the average of 6 to 8 rats in each group ± SEM *$p < 0.05$, **$p < 0.01$, ****$p < 0.0001$

Effect of BM-MSCs transplantation on the expression of the POI rats' ovarian histopathological findings and morphometry

The control rats demonstrated normal ovarian architecture. The ovarian surface showed simple squamous germinal epithelium and underlying thin tunica albuginea. The cortical regions displayed the various stages of follicular development embedded in a loose connective tissue stroma (Fig. 10A). The primordial follicles consisted of primary oocytes with eccentric pale nuclei and cytoplasm enclosed by simple squamous granulosa cells. The primary follicles were formed of primary oocytes with large pale nuclei and cytoplasm surrounded by simple cuboidal granulosa cells (Fig. 10B). The secondary follicles showed stratified polyhedral granulosa cells, well-defined eosinophilic zona pellucida, and numerous small liquor folliculi-filled clefts and theca folliculi cells (Fig. 10C). A single large antrum, stratum granulosum, and theca folliculi characterized the tertiary follicles. The latter consisted of large pale staining theca interna cells and a fibrous theca externa (Fig. 10D). The corpora lutea demonstrated large granulosa lutein cells with copious eosinophilic cytoplasm and pale, round nuclei intermingled with small theca lutein cells with intensely basophilic nuclei (Fig. 10E). The medulla was comprised of richly vascularized loose connective stroma (Fig. 10F). Regarding the POI group, the primary histopathological alterations were a simple cuboidal germinal epithelium, thick tunica albuginea, cortical stromal hypercellularity, and degenerated ovarian follicles. These follicles displayed shrunken oocytes with darkly stained nuclei and cytoplasm (Fig. 8H), ill-defined zona pellucida. The granulosa and theca interna cells appeared loosely arranged, shrunken, and pyknotic, with granular antral fluid (Fig. 10I, J). The degenerated corpus luteum (CL) had irregularly shaped granulosa lutein with pyknotic nuclei and large gaps between them (Fig. 10K). The medulla showed a prominent increase in cellularity with congested blood vessels and vascular wall thickening (Fig. 10L). In the POI + BM-MSCs group, mild ovarian cortical and medullary cellularity with moderate thickness of tunica albuginea was noticed. The developing follicles appeared nearly normal with mild vascular congestion (Fig. 10M – R). These data were statistically confirmed. The number of degenerated primordial, primary, secondary, and tertiary follicles was significantly higher in the POI group than in the control group. Post-BM-MSCs transplantation in the POI rats significantly reduced this number compared to the POI (Fig. 11A – F). Compared with the control group, the thickness of tunica

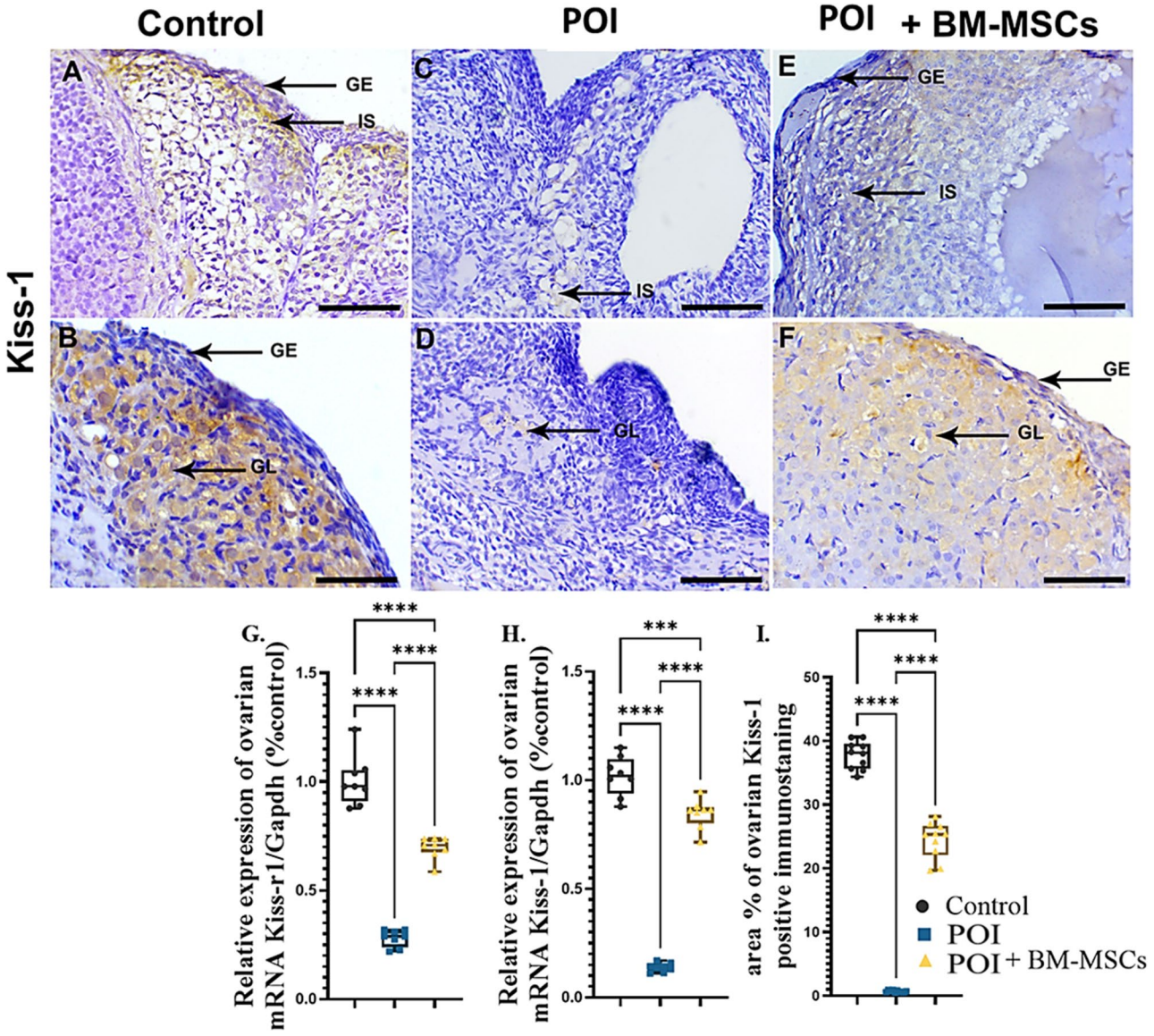

Fig. 8 Effect of BM-MSCs transplantation on the expression of ovarian Kisspeptin system of the POI rats (**A** – **I**). Representative images from the anti-Kiss1 protein immunostained rat ovarian section of the CON (**A**, **B**), POI (**C**, **D**), and POI + BM-MSCs groups (**E**, **F**) lower and higher magnification, respectively, showing cytoplasmic immune expression of germinal epithelium (GE), interstitial stromal cells (IS), and granulosa lutein cells (GL) as intense, faint, and moderate immunoreactivity in CON, POI, and POI + BM-MSCs groups, respectively. Scale bars **A**, **C**, **E** = 200 µm; **B**, **D**, **F** = 50 µm, **G**. Relative expression of ovarian mRNA Kiss-r1, H. Relative expression of ovarian mRNA Kiss-1, and **I**. Area % of ovarian Kiss-1 positive immunostaining. The values represent the average of 6 to 8 rats in each group ± SEM *$p < 0.05$, **$p < 0.01$, ***$p < 0.001$, ****$p < 0.0001$

albuginea and the number of ovarian interstitial fibroblast cells was significantly increased in the POI group. On the other hand, these parameters were significantly decreased in the POI + BM-MSCs group compared to the POI group (Fig. 11A – F).

Discussion

POI is a clinical disease that primarily impacts women who are younger than 40 years old. The absence of folliculogenesis and the subsequent production of ovarian estrogen distinguishes it. One of the most profound consequences of cancer treatment in young female patients is the development of ovarian impairment, resulting in a notable decline in reproductive capacity [35]. Consequently, researchers have been actively exploring diverse therapy methodologies to augment the quality of life for patients. Recently, many studies have been devoted to investigating mesenchymal stem cells for controlling many chronic incurable as an aid in tissue repairing and regeneration, such as bone marrow derived mesenchymal stem cells (BM-MSCs) [1]. Recently, Long and short non-coding RNA play pivotal role either in

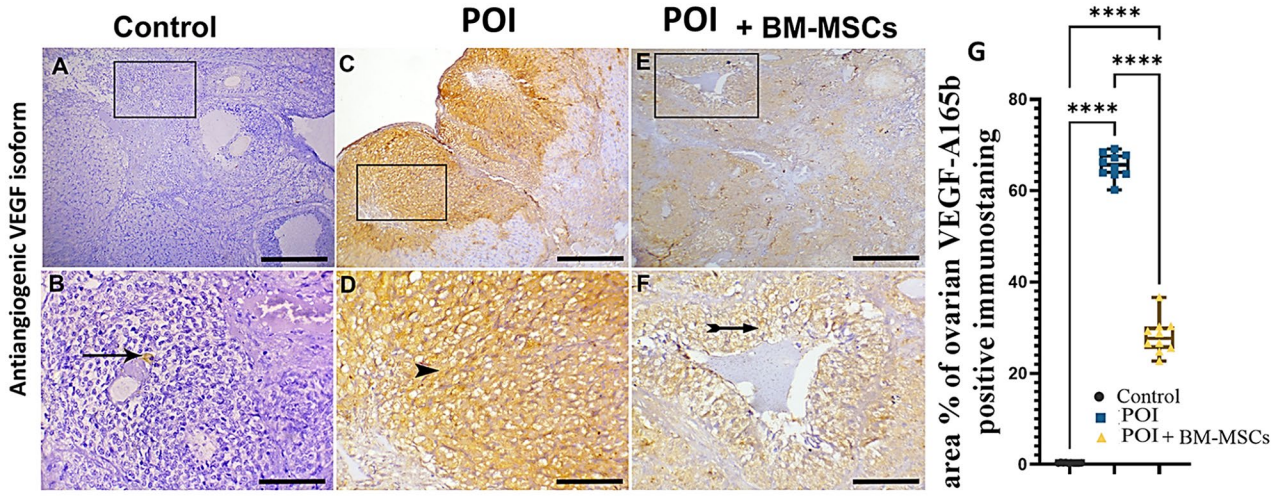

Fig. 9 Effect of BM-MSCs transplantation on the expression of ovarian anti-angiogenic VEGF-A 165b isofrm of the POI rats (**A** – **G**). Representative images from the anti-angiogenic VEGFA 165b isoform immunostained rat ovarian section of the CON (**A**), POI (**C**), and POI + BM-MSCs groups (**E**) and their respective higher magnifications (**B**, **D**, **F**). Notice faint (arrow), intense (arrowhead), and moderate (biforked arrow) cytoplasmic immunoreactivities in the granulosa lutein cells of the CON, POI, and POI + BM-MSCs groups, respectively. Scale bars **A**, **C**, **E** = 200 µm; **B**, **D**, **F** = 50 µm, and **G**. Area % of ovarian anti-angiogenic VEGFA 165b isoform positive immunostaining. The values represent the average of 6 to 8 rats in each group ± SEM *$p < 0.05$, **$p < 0.01$, ***$p < 0.001$, ****$p < 0.0001$

diseases progression or therapy, among the lncRNAs are Neat-1 and Hotair-1 which displayed anti-apoptotic activity via sponging the pro-apoptotic miRNAs mir-125a and mir-34a respectively [15–17]. Additionally, several microRNAs exerted anti-apoptotic properties such as mir-21 [26], mir-144 [15], and mir-664 [16] via augmenting the expression of P53 and caspases. MSCs secretome containing many lncRNAs and microRNAs which are involved in their regenerative mechanisms [24, 25]. However, the role of MSCs' Hotair-1, Neat-1, mir-21-5p, mir-144-5p, and mir-664-5p in regeneration of the ovarian injury as well as their effect on both peripheral and central kisspeptin system in recovery of the ovarian insufficiency remains elusive. Thus, the present study was designed to explore the underlying mechanism of BM-MSCs in recovery of the premature ovarian insufficiencyregarding the role of MSCs' lncRNA (Neat-1 and Hotair-1) and microRNAs (mir-21-5p, mir-144-5p, and mir-664-5p) on ovarian granulosa cell apoptosis in addition exploring BM-MSCs effect on IGF-1 – kisspeptin system either peripherally or centrally.

The homing capacity of mesenchymal stem cells (MSCs) is a crucial determinant in assessing the efficacy of MSC-based therapy [36, 37]. The result of the present investigation revealed that the intraperitoneal transplanted BM-MSCs homed to the injured ovarian tissue, which was noticed via detecting expression of SRY mRNA expression of the male rats BM-MSCs within the POI female rat ovaries that double confirmed via detecting red fluorescence emission of the PKH-26 within the POI female rat ovaries. The intraperitoneal route was selected in order to mitigate the risk of pulmonary entrapment and apoptosis of the infused BM-MSCs, as found with the intravenous administration approach. The intravenous administration method limits the accessibility of transplanted MSCs in the injured tissues, since almost of the trapped MSCs are undergo apoptosis and only 3% of the infused cells are redistributed to the site of injury [38]. In the current study, a rat POI model was established by administration of Cyclophosphamide. The results indicated that Cyclophosphamide successfully induced POI and significantly reduced the number of follicles at various stages of development [39]. The current findings also showed that the ovarian stroma cells and medulla were destroyed, along with leakage, edema, and affection on the blood vessels. The ovarian stroma's distortion is caused by this toxic impact of the Cyclophosphamide [4]. Our study revealed that in the (POI + BM – MSCs) group, the follicle number was nearly restored to normal at all stages (primordial, primary, secondary, and antral follicle) [4].

Reactive oxygen species (ROS) are generated by the H2O2 and NADPH oxidase system as part of cellular metabolism. These ROS are counteracted by antioxidant system which aid in their elimination and the imbalance in those system will induce the oxidative stress [40]. Oxidative stress causes DNA damage and mutation, protein oxidation, mitochondrial damage, and lipid peroxidation, all impairing biological processes and ultimately causing cell aging and death [41]. The findings of the existing study illustrated that cyclophosphamide-induced ovarian oxidative stress was noticed with a significant elevation in the lipid peroxidation markers MDA and reduction in the CAT, SOD, TAC, and GSH enzymes. These explain

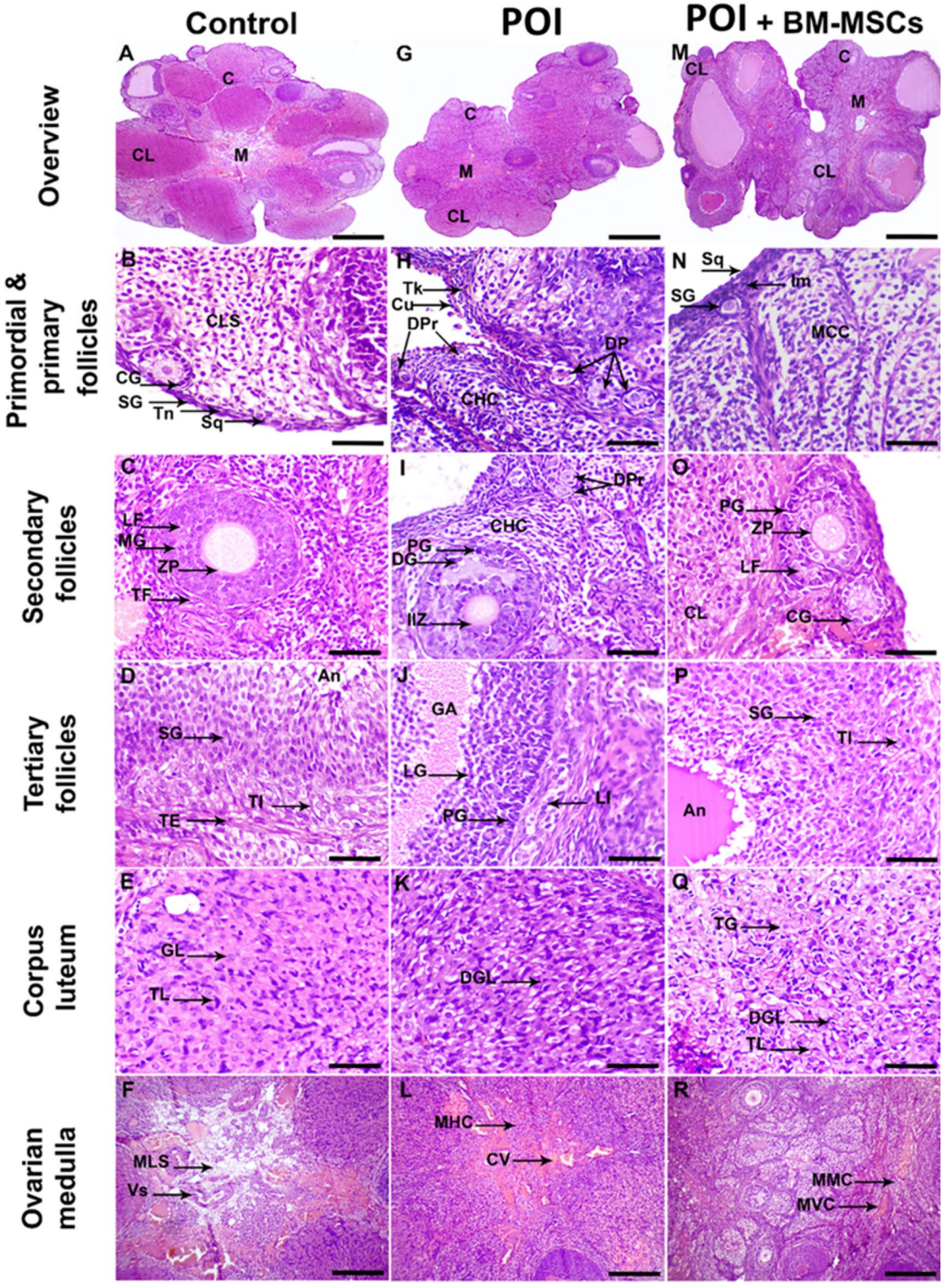

Fig. 10 (See legend on next page.)

that Cyclophosphamide induces POI via accelerating lipid peroxidation of the ovarian mucosal tissue, rendering the antioxidant system unable to neutralize ROS [42]. Therefore, excessive ROS accumulation induces infertility by delaying oocyte maturation and causing granulosa cell apoptosis [43].

The findings of the present investigation indicate that the treatment of BM-MSCs led to a notable reduction in

(See figure on previous page.)

Fig. 10 Effect of BM-MSCs transplantation on the expression of ovarian histopathological findings of the POI rats (**A** – **R**). Representative **H**&**E** images of CON (A, B, C, D, E, F), POI (G, H, I, J, K, L), and POI + BM-MSCs (M, N, O, P, Q, R) rat ovarian tissue. Control group: **B**: Squamous germinal epithelium (SG) and thin tunica albuginea (Tn). Cortex (**C**) with loose connective tissue stroma (CLS) housing primordial follicles comprising primary oocyte with an eccentric pale nucleus and cytoplasm enclosed by simple squamous granulosa cells (Sq). Primary follicle (PF) containing primary oocyte with a large pale nucleus and cytoplasm enclosed by simple cuboidal granulosa cells (CG). **C**: Secondary follicle composed of stratified granulosa cells with mitotic figures (MG), well-defined, eosinophilic zona pellucida (ZP), small liquor folliculi-filled clefts (LF) and theca folliculi (TF). **D**: Tertiary follicle with single antrum (An), stratum granulosum (SG) enclosed by large pale staining cells of theca interna (TI) and fibrous theca externa (TE). **E**: Corpora lutea (CL) showing large eosinophilic granulosa lutein cells (GL) intermingled with small intensely stained theca lutein cells (TL). **F**: Ovarian medulla (M) demonstrates richly vascularized (V) loose CT stroma (MLS). POI Group: **H**: Cuboidal germinal epithelium (Cu), thick tunica albuginea (Tk), cortical interstitial stroma hypercellularity (CHC), degenerated primordial (DPr), primary (DP), **I**: secondary and, **J**: tertiary follicles with indistinct zona pellucida (IZ), pycnotic (PG), shrunken and loosely arranged granulosa (LG) and theca interna cells (LI) and granular antral fluid (GA). **K**: Degenerated CL shows irregular-shaped granulosa lutein cells with pyknotic nuclei separated by large gaps (DGL). **L**: Medullary ovarian Hypercellular (MHC) with thickened, congested blood vessels (CV). POI + BM-MSCs group: **N**: Tunica albuginea of intermediate thickness (Im) and mild cortical interstitial stroma hypercellularity (MCC). **O**, **P**, **Q**: Nearly normal follicles and corpus luteum. **R**: Mild medullary cellularity (MMC) with mild vascular congested blood vessels (MVC). Scale bars A, G, M = 400 µm; B, C, D, E, H, I, J, K,N, O, P, Q = 40 µm, F, L, *R* = 150 µm

the ovarian peroxidation marker MDA, as well as an elevation in the antioxidant activity of SOD, CAT, TAC, and GSH. These findings demonstrate the antioxidant activity of the BM-MSCs which could be attributed to the of many soluble trophic factor in MSCs' secretome such as HGF, IL-6, IL-8, VEGF, and LIF, in conjunction with the initiation of the FOXO-PI3K/AKT and Nrf2-ARE signaling pathways [44].

Along with the oxidative stress-induced-ovarian granulosa cell apoptosis, there are many miRNAs such as mir-125a and mir34a that activate P53 and caspases cascade, thus, aggravating ovarian cell apoptosis [45, 46]. The results of the present study were in accordance with the previous notions, as the POI group showed a sharp upregulation in the expression of the ovarian mir-125a and mir-34a with a noticeable upregulation in the expression of the pro-apoptotic markers P53 and caspase-3 and downregulation in the antiapoptotic marker BCL-2 and Notch-1, that obviously reflects the negative regulatory role of the mir-125a for BCL-2 [47] and mir-34a [48] for Notch-1 expression subsequently, activate ovarian granulosa cell apoptosis. Interestingly, BM-MSCs transplantation in the POI rat model exerted a marked downregulation in the expression of the mir-125a and mir-34a accompanied by upregulation of BCL-2 and Notch-1 which illustrated that BM-MSCs hindering the pro-apoptotic activity of the mir-125a and mir-34a. On the other hand, the results showed that the expression of the lncRNAs neat-1 and Hotair-1 was upregulated in the BM-MSCs and their conditioned media. The presence of Neat-1 and Hotair-1 in the conditioned media of BM-MSCs clearly evidenced that the above-mentioned lncRNAs are a part of their secretome which is in accordance with a previous report [25] which stated that the MSCs secretome includes proteins, DNA, tRNA, and lncRNAs. Besides, the findings revealed a significant downregulation in the expression of the ovarian Neat-1 and Hotair-1 together with an upstream regulation in the ovarian pro-apoptotic markers, mir-125a, and mir-34a in POI rats which evidently proves the role of these lncRNA in regulation the cellular apoptosis [49, 50]. On the contrary, BM-MSCs-treated POI rats displayed a significant upregulation in the expression of the lncRNAs; Hotair-1 and Neat-1 compared with the POI group, and according to the previous findings of [7, 21] reported that Hotair-1 sponge mir-34a and [22] stated that Neat-1 sponge mir-125a, the present findings suggested that BM-MSCs could alleviate the ovarian cell apoptosis via their secretome that embraced Neat-1 and Hotair-1 which masked the apoptotic effect of the proapoptotic mir-125a and mir-34a respectively and upregulating the antiapoptotic markers BCL-2 and Notch-1 improve ovarian cell viability and inhibited their death.

Furthermore, the result of the current investigation illustrated that the BM-MSCs and their conditioned media showed a marked expression of mir-21-5p, mir-144-5p, and mir-664-5p which represents another part of the MSCs secretome that exhibited a proven antiapoptotic activity via diminishing expression of P53 and caspases [10–12, 19, 26, 27], also, the result of the in *vivo* study confirm that in *vitro* findings as the POI group showed significant downregulation in the expression of mir-21-5p, mir-144-5p, and mir-664-5p in consort with upregulation in the expression of P53 and Caspase-3 compared with the control group, however, BM-MSCs treated POI group showed a contrary situation compared with the POI group, which suggesting another antiapoptotic mechanism of BM-MSCs via secreting extracellular vesicle comprehend several microRNAs mir-21-5p, mir-144-5p, mir-664-5p that counter act the ovarian cells apoptotic signals via a paracrine effect.

The HPG axis governs the regulation of reproduction. The release of GnRH serves to orchestrate the hypothalamic regulation of sexual activity [51]. Recent research has revealed that the upstream regulator of pulsatile and surge GnRH is kisspeptin (Kiss1). On the other side, the presence of kisspeptin immunoreactivity has been detected in steroidogenic granulosa lutein cells, with its levels progressively increasing in accordance with the advancing development of the corpus luteum

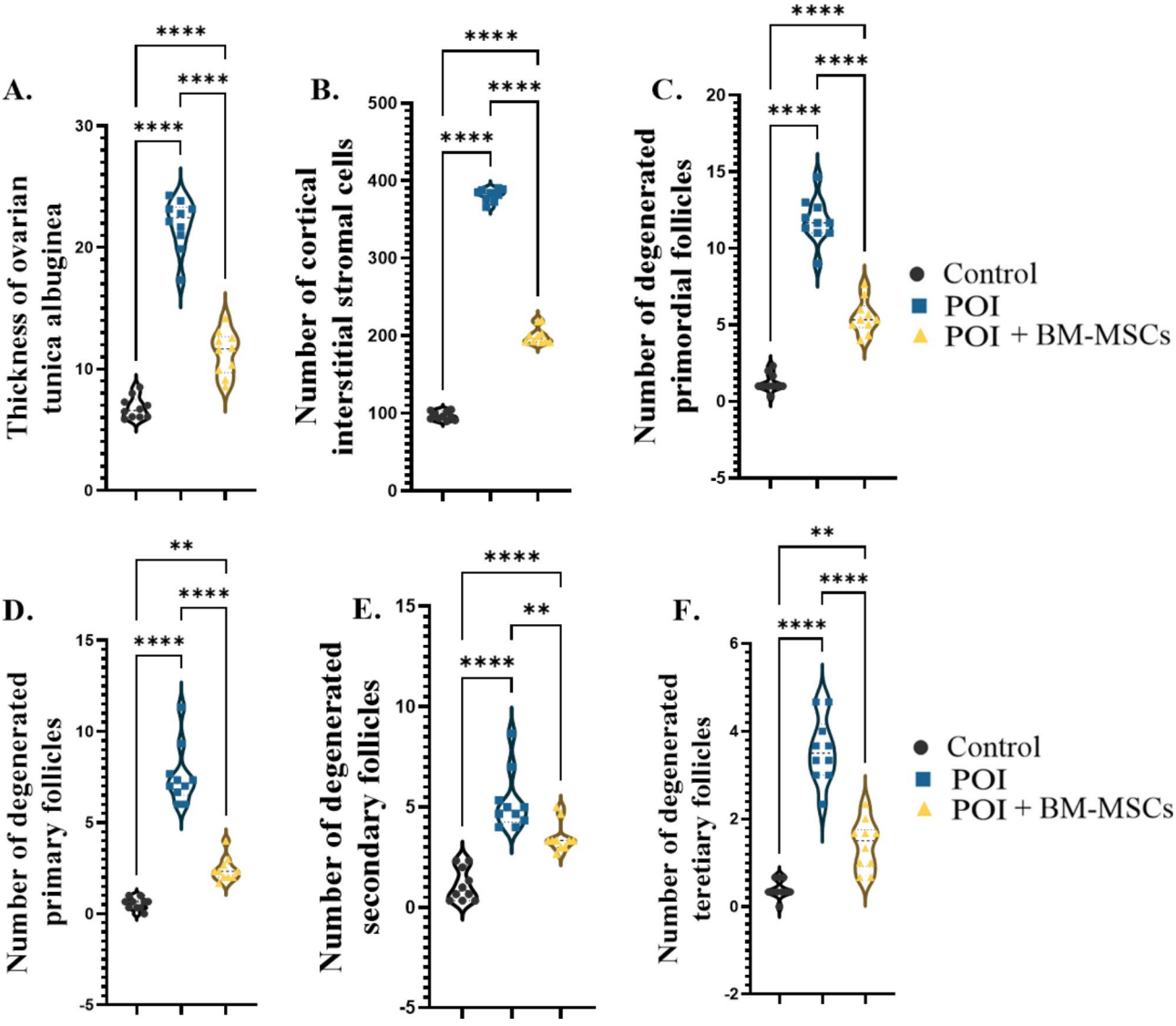

Fig. 11 Effect of BM-MSCs transplantation on the expression of ovarian histopathological morphometry of the POI rats (**A** – **F**). **A**. Thickness of ovarian tunica albuginea, **B**. Number of cortical stromal cells, **C**. Number of degenerated primordial follicles, **D**. Number of degenerated primary follicles, **E**. Number of degenerated secondary follicles, and **F**. Number of degenerated tertiary follicles. The values represent the average of 6 to 8 rats in each group ± SEM
*$p < 0.05$, **$p < 0.01$, ***$p < 0.001$, ****$p < 0.0001$

[52]. According to an earlier study, kisspeptin increases the transcription of the main steroidogenic enzymes CYP11A, StAR, and 3β-HSD [53]. Additionally, kisspeptin dramatically increases the luteal cells' ability to produce progesterone [54]. Recent data show that specific actions of kisspeptins are obligatory for maintaining full ovulatory capacity throughout the reproductive life span and preventing excessive atresia of large antral follicles [55]. The dysfunction of the kisspeptin/ Kiss-1r system causes POI, which is characterized by a premature regression in ovulatory rate, progressive oocyte, antral follicle loss, and infertility [5]. The result of the present work showed significant downregulation of hypothalamic Kiss-1, GnRH, Kiss-1r, hypophyseal GnRhr, ovarian Kiss-1, Kiss-1r, and upregulation of GnIH in the POI group when compared with the control group, which could be attributed to the oxidative stress induced by cyclophosphamide administration [56]. On the contrary, the results revealed a significant upregulation in gene expression of hypothalamic Kiss-1, Kiss-1r, GnRH, hypophyseal GnRH, and ovarian Kiss-1 and a decrease of GnIH in the POI+BM – MSCs group compared with the POI group [57]. Additionally, the immunohestochemical analysis of the ovarian tissue confirmed the molecular finding as the POI group showed a marked downregulation in the expression of Kiss-1 positive immunostained cells, however, the BM-MSCs treated POI group showed the reverse situation. These findings, endorse the

modulatory role of BM-MSCs for the peripheral and central kisspeptin system as well as HPG axis, which might be owed to secretory activity of the BM-MSCs for several growth factors such as IGF-1 [58, 59]. On the same context, the results revealed a significant upregulation in the expression of ovarian and hypothalamic IGF-1 of BM-MSCs treated POI rats, which is downregulated in POI groups, IGF-1 could improve the kisspeptin production as both the ovarian and hypothalamic kiss-1 secreting cells expressed the insulin growth factor receptors (IGFR) which is indispensable improving energy production in those cells hence, increasing their secretory activity for kisspeptin-1, improving gonadotrophin secretion, and ovarian steroidogenesis [57, 60] Furthermore, IGF can modify theca or granulosa cells' responsiveness to gonadotropin activation [61] and improve their differentiation and proliferation by enhancing the FSH function in granulosa cells [62]. Too, IGF level inhibits AMH function, which reduces the growth and performance of antral and preantral follicles. Thereby, IGF can control folliclogensis [63]. Additionally, BM-MSCs could improve fertility by downregulating the expression of gonadotrophin inhibiting hormone (GnIH) which reported by Khamis T, Hegazy AA, El-Fatah SSA, Abdelfattah ER, Abdelfattah MMM, Fericean LM and Arisha AH [64] who reported that breast milk mesenchymal stem cells transplantation downregulated the expression of GnIH and improving HPG axis in diabetic infertility rat model.

On the other hand, ovarian granulosa express glucagon like peptide-1 receptors (GLP-1R) on their membrane [65]. GLP-1/PPAR-α influences the ovarian energy balance and promotes fatty acid oxidation [66]. Therefore, we hypothesize that GLP-1/GLP-1R is crucial for controlling granulosa cells' function and regulating ovarian steroidogenesis. In the POI model, Cyclophosphamide significantly downregulated ovarian GLP-1. PPAR-α affects ovarian cell metabolism and enhances oxidative stress by augmenting the cellular antioxidant system thus, flaring the reactive oxygen and nitrogen species, which induce inflammation and apoptosis within the ovaries [57]. Remarkably, BM-MSCs transplantation in POI female rats sharply upregulated the expression of ovarian GLP-1 and PPAR-α, indicating a favorable impact on ovarian metabolism. Several previous studies showed that improving the expression of the GLP-1 – GLP-1r/PPAR-α system enhances ovarian metabolism with a positive energy balance that abrogates ovarian dysfunction and damage [65, 67].

Moreover, the result of the present investigation illustrated that the POI group showed a significant decrease in FSH, LH, and E2 and an increase in PRL serum levels [68]. However, BM–MSCs transplantation significantly enhanced the serum FSH, LH, E2, and PRL, which clearly illustrated that BM-MSCs enhanced folliculogenesis and ovarian activity that was in the same line with Guo C, Ma Y, Situ Y, Liu L, Luo G, Li H, Ma W, Sun L, Wang W, Weng Q, Wu L and Fan D [69]. Furthermore, the results of this study showed that the POI group displayed a significant downregulation in the steroidogenic genes that include STAR, CYP17A1, CYP11A1, HSD17B, and CYP19A1 compared with the control group, which could be owed to oxidative stress-induced ovarian inflammatory and apoptotic microenvironment that in turn reduce and/or switch off ovarian steroidogenesis pathway [64]. Surprisingly, BM – MSCs infusion in POI female rats restored the abovementioned ovarian steroidogenesis-related genes in accordance [70].

The enhancement in ovarian steroidogenesis could be discussed as BM-MSCs create a local anti-inflammatory microenvironment via secreting many soluble, trophic, and anti-inflammatory factors that reduce further ovarian damage [71]. The most crucial mechanism through which MSCs reestablish ovarian function is their anti-inflammatory action since MSCs may prevent lymphocyte activation and growth, hinder the release of pro-inflammatory cytokines, and send regulatory signals to immune cells [72].

Likewise, the process of creating and remodeling the vascular system in the ovary is a fundamental aspect of ovarian development and functional recovery. This is because the follicles and CL rely on the ovarian blood vessels for nutritional support and the transportation of hormones to specific organs. The most significant stromal cells in the ovary are the ovarian granulosa cells, which provide the nutrients required for oocyte growth and follicle maturity. These cells also regulate gonadotropins, which modulate oocyte maturation through autocrine and paracrine pathways [73]. Also, Angiogenesis is governed by a group of proteins called the vascular endothelial growth factor-A (VEGFA) family. Notably, these proteins exist in two isoforms, namely proangiogenic (VEGF165) and anti-angiogenic (VEGF165b), which are generated through alternative splicing mechanisms [74]. Notably, the result of current work showed that cyclophosphamide-induced overexpression of VEGF165b in the rat ovary revealed a functional role for this isoform in delaying the development of the CL and maturation of follicles from primary to secondary to mature follicles, which in turn led to a fertility defect in these rats [75]. However, BM-MSCs administration downregulated the immunohistochemical expression of VEGF165b isoform that restored the balance between proangiogenic and anti-angiogenic VEGF, therefore restoring angiogenesis and follicular development [76], this effect could be attributed to the paracrine signaling of BM-MSCs which promote the ovarian angiogenesis and suppress ovarian inflammation, apoptosis, and fibrosis by secreting various growth factors as VEGF which increase vascularity

of the ovarian tissues [36]. On the same ground, a study conducted by researchers revealed the presence of bone marrow-derived mesenchymal stem cells (BM-MSCs) within the vasculature of damaged ovaries [6], suggesting that MSCs can impede germ cell (GC) apoptosis and stimulate GC proliferation by secretion of cytokines such as VEGF, HGF, and IGF-1. This mechanism enhances the proliferation of ovarian stem cell niches and suppresses apoptosis [76, 77]. The angiogenic potential of BM-MSCs plays a pivotal role in ovarian regeneration and restoration of fertility. In addition to evaluating the anti-angiogenic VEGF-A165b isoform, assessing the expression of vascular markers such as alpha-smooth muscle actin (α-SMA) could provide further insights into the mechanisms underlying BM-MSC-mediated ovarian vascularization [78, 79]. Other reports demonstrated that α-SMA, a marker of vascular smooth muscle cells and pericytes, is crucial for angiogenesis and vascular stabilization. Incorporating α-SMA expression analysis could elucidate the roles of BM-MSCs in promoting ovarian vascular remodeling and stabilization [78, 80]. Furthermore, the pro-angiogenic effects of mesenchymal stem cells, mediated by the secretion of various factors, including VEGF. Exploring the paracrine mechanisms through which BM-MSCs modulate ovarian angiogenesis could further substantiate their therapeutic potential in addressing ovarian insufficiency and infertility [81, 82]. Collectively, these complementary approaches would provide a comprehensive understanding of the angiogenic capacity of BM-MSCs and their implications in ovarian regeneration and fertility restoration [83, 84].

Conclusions

BM-MSCs could abate cyclophosphamide-induced ovarian insufficiency in female rats via their Neat-1, Hotair-1, mir-21-5p, mir-144-5p, and mir-664-5p rich secretome that suppress ovarian granulosa cell apoptosis via a paracrine mechanism along with improving peripheral and central IGF-1–kisspeptin system and ovarian angiogenesis.

Acknowledgements
The authors would like to thank AlMaarefa University, Riyadh, Saudi Arabia for supporting this research., and the APC was funded by the University of Life Sciences "King Mihai I" from Timisoara (ULST), Timisoara, Romania.

Author contributions
All authors shared in designing the study, methodology, data collection and analysis, statistical analysis, and writing the manuscript. All authors have read and agreed to the published version of the manuscript.

Data Availability
Data will be provided upon reasonable request from the corresponding authors.

Declarations

Ethics approval and consent to participate
All rats received humane care and the experimental methods were approved by the Institutional Animal Care and Use Committee of Badr University in Cairo (No. BUC-IACUC/VET/128/A/2022).

Competing interests
The authors declare no competing interests.

Author details
[1]Department of Biochemistry, Faculty of Veterinary Medicine, Zagazig University, Zagazig 44519, Egypt
[2]Department of Human and Clinical Anatomy, College of Medicine and Health Sciences, Sultan Qaboos University, Muscat, Sultanate of Oman
[3]Human Anatomy and Embryology Department, Faculty of Medicine, Mansoura University, Mansoura, Egypt
[4]College of Science and Health Profession, King Saud bin Abdulaziz University for Health Sciences (KSAU-HS), Riyadh, Saudi Arabia
[5]King Abdullah International Medical Research Center, Riyadh, Saudi Arabia
[6]Department of Basic Medical Sciences, College of Science and Health Professions (COSHP), King Saud bin Abdulaziz University for Health Sciences, Riyadh, Kingdom of Saudi Arabia
[7]Medical biochemistry Department, Faculty of Medicine, Zagazig University, Zagazig 44519, Egypt
[8]Medical Biochemistry and Molecular Biology Department, Faculty of Medicine, Cairo University, Cairo, Egypt
[9]Human Anatomy and Embryology Department, Faculty of Medicine, Zagazig University, Zagazig 44519, Egypt
[10]Department of Medical Biochemistry and Molecular Biology, Faculty of Medicine, Badr University in Cairo, Badr City 11829, Egypt
[11]Department of Histology and Cytology, Faculty of Veterinary Medicine, Zagazig University, Zagazig 44519, Egypt
[12]Obstetrics and Gynecology Department, Faculty of Medicine, Zagazig University, Zagazig 44519, Egypt
[13]Department of Anatomy, College of Medicine, Taibah University, Medina, Saudi Arabia
[14]Department of Anatomy, Faculty of Medicine, University of Jeddah, Jeddah, Saudi Arabia
[15]Department of Basic Medical Sciences, College of Medicine, AlMaarefa University, P.O.Box 71666, Riyadh 11597, Saudi Arabia
[16]Department of Anatomy and Embryology, Faculty of Medicine, Mansoura University, Mansoura 35516, Egypt
[17]Department of Animal Production and Veterinary Public Health, Faculty of Veterinary Medicine, University of Life Sciences, "King Mihai I" from Timisoara [ULST], Aradului St. 119, Timisoara 300645, Romania
[18]Department of Animal Physiology and Biochemistry, Faculty of Veterinary Medicine, Badr University in Cairo, Badr City 11829, Egypt
[19]Department of Physiology and Laboratory of Biotechnology, Faculty of Veterinary Medicine, Zagazig University, Zagazig 44511, Egypt
[20]Department of Pharmacology and Laboratory of Biotechnology, Faculty of Veterinary Medicine, Zagazig University, Zagazig 44519, Egypt

Received: 1 November 2023 / Accepted: 14 August 2024
Published online: 12 September 2024

References

1. Esfandyari S, Chugh RM, Park H-S, Hobeika E, Ulin M, Al-Hendy A. Mesenchymal stem cells as a Bio Organ for treatment of female infertility. Cells. 2020;9:2253.
2. Chang Z, Zhu H, Zhou X, Zhang Y, Jiang B, Li S, Chen L, Pan X, Feng X-L. Mesenchymal stem cells in Preclinical Infertility Cytotherapy: a retrospective review. Stem Cells Int. 2021;2021:8882368–8882368.
3. Yoon SY. Mesenchymal stem cells for restoration of ovarian function. Clin Experimental Reproductive Med. 2019;46:1–7.
4. Ling L, Feng X, Wei T, Wang Y, Wang Y, Wang Z, Tang D, Luo Y, Xiong Z. Human amnion-derived mesenchymal stem cell (hAD-MSC) transplantation improves ovarian function in rats with premature ovarian insufficiency

(POI) at least partly through a paracrine mechanism. Stem Cell Res Ther. 2019;10:46–46.
5. Gaytan F, Garcia-Galiano D, Dorfman MD, Manfredi-Lozano M, Castellano JM, Dissen GA, Ojeda SR, Tena-Sempere M. Kisspeptin receptor haplo-insufficiency causes premature ovarian failure despite preserved gonadotropin secretion. Endocrinology. 2014;155:3088–97.
6. Liu J, Zhang H, Zhang Y, Li N, Wen Y, Cao F, Ai H, Xue X. Homing and restorative effects of bone marrow-derived mesenchymal stem cells on cisplatin injured ovaries in rats. Mol Cells. 2014;37:865–72.
7. Alanazi A, Alassiri M, Jawdat D, Almalik Y. Mesenchymal stem cell therapy: a review of clinical trials for multiple sclerosis. Regen Ther. 2022;21:201–9.
8. Wei X, Yang X, Han Z-p, Qu F-f, Shao L. Shi Y-f: mesenchymal stem cells: a new trend for cell therapy. Acta Pharmacol Sin. 2013;34:747–54.
9. Zhao Y-X, Chen S-R, Su P-P, Huang F-H, Shi Y-C, Shi Q-Y, Lin S. Using Mesenchymal Stem Cells to Treat Female Infertility: An Update on Female Reproductive Diseases. *Stem cells international* 2019, 2019:9071720–9071720.
10. Sheriff L, Alanazi A, Ward LSC, Ward C, Munir H, Rayes J, Alassiri M, Watson SP, Newsome PN, Rainger GE, et al. Origin-specific adhesive interactions of mesenchymal stem cells with platelets influence their Behavior after infusion. Stem Cells. 2018;36:1062–74.
11. Alanazi A, Munir H, Alassiri M, Ward LSC, McGettrick HM, Nash GB. Comparative adhesive and migratory properties of mesenchymal stem cells from different tissues. Biorheology. 2019;56:15–30.
12. Iyer MK, Niknafs YS, Malik R, Singhal U, Sahu A, Hosono Y, Barrette TR, Prensner JR, Evans JR, Zhao S, et al. The landscape of long noncoding RNAs in the human transcriptome. Nat Genet. 2015;47:199–208.
13. Fitzgerald JB, George J, Christenson LK. Non-coding RNA in Ovarian Development and Disease. Adv Exp Med Biol. 2016;886:79–93.
14. Zheng C, Liu S, Qin Z, Zhang X, Song Y. LncRNA DLEU1 is overexpressed in premature ovarian failure and sponges miR-146b-5p to increase granulosa cell apoptosis. J Ovarian Res. 2021;14:151.
15. Zhao W, Dong L. Long non-coding RNA HOTAIR overexpression improves premature ovarian failure by upregulating Notch-1 expression. Exp Ther Med. 2018;16:4791–5.
16. Ding N, Wu H, Tao T, Peng E. NEAT1 regulates cell proliferation and apoptosis of ovarian cancer by miR-34a-5p/BCL2. Onco Targets Ther. 2017;10:4905–15.
17. Liu X, Shang W, Zheng F. Long non-coding RNA NEAT1 promotes migration and invasion of oral squamous cell carcinoma cells by sponging microRNA-365. Exp Ther Med. 2018;16:2243–50.
18. Li M, Peng J, Zeng Z. Overexpression of long non-coding RNA nuclear enriched abundant transcript 1 inhibits the expression of p53 and improves premature ovarian failure. Exp Ther Med. 2020;20:69.
19. Yang M, Lin L, Sha C, Li T, Zhao D, Wei H, Chen Q, Liu Y, Chen X, Xu W, et al. Bone marrow mesenchymal stem cell-derived exosomal mir-144-5p improves rat ovarian function after chemotherapy-induced ovarian failure by targeting PTEN. Lab Invest. 2020;100:342–52.
20. Liu T, Lin J, Chen C, Nie X, Dou F, Chen J, Wang Z, Gong Z. MicroRNA-146b-5p overexpression attenuates premature ovarian failure in mice by inhibiting the Dab2ip/Ask1/p38-Mapk pathway and γH2A.X phosphorylation. Cell Prolif. 2021;54:e12954.
21. Shao T, Hu Y, Tang W, Shen H, Yu Z, Gu J. The long noncoding RNA HOTAIR serves as a microRNA-34a-5p sponge to reduce nucleus pulposus cell apoptosis via a NOTCH1-mediated mechanism. Gene. 2019;715:144029.
22. Yan H, Liang H, Liu L, Chen D, Zhang Q. Long noncoding RNA NEAT1 sponges miR–125a–5p to suppress cardiomyocyte apoptosis via BCL2L12. Mol Med Rep. 2019;19:4468–74.
23. He Y, Chen D, Yang L, Hou Q, Ma H, Xu X. The therapeutic potential of bone marrow mesenchymal stem cells in premature ovarian failure. Stem Cell Res Ther. 2018;9:263–263.
24. Baglio SR, Rooijers K, Koppers-Lalic D, Verweij FJ, Pérez Lanzón M, Zini N, Naaijkens B, Perut F, Niessen HW, Baldini N, Pegtel DM. Human bone marrow- and adipose-mesenchymal stem cells secrete exosomes enriched in distinctive miRNA and tRNA species. Stem Cell Res Ther. 2015;6:127.
25. Lai RC, Tan SS, Yeo RW, Choo AB, Reiner AT, Su Y, Shen Y, Fu Z, Alexander L, Sze SK, Lim SK. MSC secretes at least 3 EV types each with a unique permutation of membrane lipid, protein and RNA. J Extracell Vesicles. 2016;5:29828.
26. Cheng X, Zhang G, Zhang L, Hu Y, Zhang K, Sun X, Zhao C, Li H, Li YM, Zhao J. Mesenchymal stem cells deliver exogenous miR-21 via exosomes to inhibit nucleus pulposus cell apoptosis and reduce intervertebral disc degeneration. J Cell Mol Med. 2018;22:261–76.
27. Sun B, Ma Y, Wang F, Hu L, Sun Y. Mir-644-5p carried by bone mesenchymal stem cell-derived exosomes targets regulation of p53 to inhibit ovarian granulosa cell apoptosis. Stem Cell Res Ther. 2019;10:360.
28. Smajilagić A, Aljičević M, Redžić A, Filipović S, Lagumdžija A. Rat bone marrow stem cells isolation and culture as a bone formative experimental system. Bosnian J Basic Med Sci. 2013;13:27–30.
29. Gabr H, Rateb MA, El Sissy MH, Ahmed Seddiek H, Ali Abdelhameed Gouda S. The effect of bone marrow-derived mesenchymal stem cells on chemotherapy induced ovarian failure in albino rats. Microsc Res Tech. 2016;79:938–47.
30. Al-Shahat A, Hulail MAE, Soliman NMM, Khamis T, Fericean LM, Arisha AH, Moawad RS. Melatonin mitigates Cisplatin-Induced Ovarian Dysfunction via altering steroidogenesis, inflammation, apoptosis, oxidative stress, and PTEN/PI3K/Akt/mTOR/AMPK signaling pathway in female rats. Pharmaceutics. 2022;14:2769.
31. Abdelbaset-Ismail A, Tharwat A, Ahmed AE, Khamis T, Abd El-Rahim IH, Alhag SK, Dowidar MF. Transplantation of adipose-derived mesenchymal stem cells ameliorates acute hepatic injury caused by nonsteroidal anti-inflammatory drug diclofenac sodium in female rats. Biomed Pharmacother. 2022;155:113805.
32. Livak KJ, Schmittgen TD. Analysis of relative gene expression data using real-time quantitative PCR and the 2 – ΔΔCT method. Methods. 2001;25:402–8.
33. Suvarna KS, Layton C, Bancroft JD. Bancroft's theory and practice of histological techniques. Elsevier health sciences; 2018.
34. Schindelin J, Arganda-Carreras I, Frise E, Kaynig V, Longair M, Pietzsch T, Preibisch S, Rueden C, Saalfeld S, Schmid B, et al. Fiji: an open-source platform for biological-image analysis. Nat Methods. 2012;9:676–82.
35. Abd-Allah SH, Shalaby SM, Pasha HF, El-Shal AS, Raafat N, Shabrawy SM, Awad HA, Amer MG, Gharib MA, El Gendy EA, et al. Mechanistic action of mesenchymal stem cell injection in the treatment of chemically induced ovarian failure in rabbits. Cytotherapy. 2013;15:64–75.
36. Li J, Mao Q, He J, She H, Zhang Z, Yin C. Human umbilical cord mesenchymal stem cells improve the reserve function of perimenopausal ovary via a paracrine mechanism. Stem Cell Res Ther. 2017;8:55–55.
37. Lin W, Xu L, Zwingenberger S, Gibon E, Goodman SB, Li G. Mesenchymal stem cells homing to improve bone healing. J Orthop Translation. 2017;9:19–27.
38. Fischer UM, Harting MT, Jimenez F, Monzon-Posadas WO, Xue H, Savitz SI, Laine GA, Cox CS Jr. Pulmonary passage is a major obstacle for intravenous stem cell delivery: the pulmonary first-pass effect. Stem Cells Dev. 2009;18:683–92.
39. Bahrehbar K, Rezazadeh Valojerdi M, Esfandiari F, Fathi R, Hassani S-N, Baharvand H. Human embryonic stem cell-derived mesenchymal stem cells improved premature ovarian failure. World J stem Cells. 2020;12:857–78.
40. Ježek P, Holendová B, Plecitá-Hlavatá L. Redox Signaling from Mitochondria: Signal Propagation and its targets. Biomolecules. 2020;10:93.
41. Ra K, Park SC, Lee BC. Female Reproductive aging and oxidative stress: mesenchymal stem cell conditioned medium as a promising antioxidant. Int J Mol Sci. 2023;24:5053.
42. Devine PJ, Perreault SD, Luderer U. Roles of reactive oxygen species and antioxidants in ovarian toxicity. Biol Reprod. 2012;86:27–27.
43. Wojsiat J, Korczyński J, Borowiecka M, Żbikowska HM. The role of oxidative stress in female infertility and in vitro fertilization. Postępy Higieny i Medycyny Doświadczalnej. 2017;71:0–0.
44. Amoroso MR, Matassa DS, Agliarulo I, Avolio R, Maddalena F, Condelli V, Landriscina M, Esposito F. Stress-adaptive response in Ovarian Cancer Drug Resistance. Stress and inflammation in disorders. Elsevier; 2017. pp. 163–98.
45. Wang C, Li D, Zhang S, Xing Y, Gao Y, Wu J. MicroRNA-125a-5p induces mouse granulosa cell apoptosis by targeting signal transducer and activator of transcription 3. Menopause. 2016;23:100–7.
46. Han S, Zhao X, Zhang Y, Amevor FK, Tan B, Ma M, Kang H, Wang J, Zhu Q, Yin H, Cui C. MiR-34a-5p promotes autophagy and apoptosis of ovarian granulosa cells via the Hippo-YAP signaling pathway by targeting LEF1 in chicken. Poult Sci. 2023;102:102374.
47. Tong Z, Liu N, Lin L, Guo X, Yang D, Zhang Q. miR-125a-5p inhibits cell proliferation and induces apoptosis in colon cancer via targeting BCL2, BCL2L12 and MCL1. Biomed Pharmacother. 2015;75:129–36.
48. Park EY, Chang E, Lee EJ, Lee HW, Kang HG, Chun KH, Woo YM, Kong HK, Ko JY, Suzuki H, et al. Targeting of miR34a-NOTCH1 axis reduced breast cancer stemness and chemoresistance. Cancer Res. 2014;74:7573–82.
49. Fang J, Zheng W, Hu P, Wu J. Investigating the effect of lncRNA HOTAIR on apoptosis induced by myocardial ischemia-reperfusion injury. Mol Med Rep 2021, 23.

50. Chai WN, Wu YF, Wu ZM, Xie YF, Shi QH, Dan W, Zhan Y, Zhong JJ, Tang W, Sun XC, Jiang L. Neat1 decreases neuronal apoptosis after oxygen and glucose deprivation. Neural Regen Res. 2022;17:163–9.
51. Acevedo-Rodriguez A, Kauffman AS, Cherrington BD, Borges CS, Roepke TA, Laconi M. Emerging insights into hypothalamic-pituitary-gonadal axis regulation and interaction with stress signalling. J Neuroendocrinol. 2018;30:e12590–12590.
52. Cao Y, Li Z, Jiang W, Ling Y, Kuang H. Reproductive functions of Kisspeptin/KISS1R systems in the periphery. Reproductive Biology Endocrinology: RB&E. 2019;17:65–65.
53. Peng J, Tang M, Zhang B-P, Zhang P, Zhong T, Zong T, Yang B, Kuang H-B. Kisspeptin stimulates progesterone secretion via the Erk1/2 mitogen-activated protein kinase signaling pathway in rat luteal cells. Fertil Steril. 2013;99:1436–e14431431.
54. Xiao Y, Ni Y, Huang Y, Wu J, Grossmann R, Zhao R. Effects of kisspeptin-10 on progesterone secretion in cultured chicken ovarian granulosa cells from preovulatory (F1–F3) follicles. Peptides. 2011;32:2091–7.
55. Ruohonen ST, Gaytan F, Usseglio Gaudi A, Velasco I, Kukoricza K, Perdices-Lopez C, Franssen D, Guler I, Mehmood A, Elo LL, et al. Selective loss of kisspeptin signaling in oocytes causes progressive premature ovulatory failure. Hum Reprod (Oxford England). 2022;37:806–21.
56. Barberino RS, Silva RLS, Palheta Junior RC, Smitz JEJ, Matos MHT. Protective effects of antioxidants on Cyclophosphamide-Induced ovarian toxicity. Biopreserv Biobank. 2023;21:121–41.
57. Khamis T, Abdelalim AF, Abdallah SH, Saeed AA, Edress NM, Arisha AH. Early intervention with breast milk mesenchymal stem cells attenuates the development of diabetic-induced testicular dysfunction via hypothalamic Kisspeptin/Kiss1r-GnRH/GnlH system in male rats. Biochim et Biophys Acta (BBA) - Mol Basis Disease. 2020;1866:165577.
58. Hou J, Peng X, Wang J, Zhang H, Xia J, Ge Q, Wang X, Chen X, Wu X. Mesenchymal stem cells promote endothelial progenitor cell proliferation by secreting insulin-like growth factor-1. Mol Med Rep. 2017;16:1502–8.
59. Youssef A, Aboalola D, Han VKM. The roles of insulin-like growth factors in mesenchymal stem cell niche. Stem Cells Int 2017, 2017:9453108–9453108.
60. Rocha AM, Ding J, Lehman M, Smith GD. Kisspeptin and kisspeptin receptor are expressed in mouse oocytes and participate in meiosis resumption. Fertil Steril. 2012;98:S22.
61. Afradiasbagharani P, Hosseini E, Allahveisi A, Bazrafkan M. The insulin-like growth factor and its players: their functions, significance, and consequences in all aspects of ovarian physiology. Middle East Fertility Soc J 2022, 27.
62. Baumgarten SC, Convissar SM, Fierro MA, Winston NJ, Scoccia B, Stocco C. IGF1R signaling is necessary for FSH-induced activation of AKT and differentiation of human cumulus granulosa cells. J Clin Endocrinol Metab. 2014;99:2995–3004.
63. Andreassen M, Frystyk J, Faber J, Kristensen LØ, Juul A. Growth hormone (GH) activity is associated with increased serum oestradiol and reduced Anti-Müllerian hormone in healthy male volunteers treated with GH and a GH antagonist. Andrology. 2013;1:595–601.
64. Khamis T, Hegazy AA, El-Fatah SSA, Abdelfattah ER, Abdelfattah MMM, Fericean LM, Arisha AH. Hesperidin mitigates Cyclophosphamide-Induced Testicular Dysfunction via altering the hypothalamic pituitary gonadal Axis and testicular steroidogenesis, inflammation, and apoptosis in male rats. Pharmaceuticals (Basel Switzerland). 2023;16:301.
65. Sun Z, Li P, Wang X, Lai S, Qiu H, Chen Z, Hu S, Yao J, Shen J. GLP-1/GLP-1R signaling regulates ovarian PCOS-Associated Granulosa cells proliferation and antiapoptosis by modification of Forkhead Box protein O1 Phosphorylation sites. Int J Endocrinol. 2020;2020:1484321–1484321.
66. Starovlah IM, Radovic Pletikosic SM, Kostic TS, Andric SA. Reduced spermatozoa functionality during stress is the consequence of adrenergic-mediated disturbance of mitochondrial dynamics markers. Sci Rep. 2020;10:16813–16813.
67. Nylander M, Frøssing S, Clausen HV, Kistorp C, Faber J, Skouby SO. Effects of liraglutide on ovarian dysfunction in polycystic ovary syndrome: a randomized clinical trial. Reprod Biomed Online. 2017;35:121–7.
68. Abdel-Aziz AM, Mohamed ASM, Abdelazem O, Okasha AMM, Kamel MY. Cilostazol protects against cyclophosphamide-induced ovarian toxicity in female rats: role of cAMP and HO-1. Toxicol Mech Methods. 2020;30:526–35.
69. Guo C, Ma Y, Situ Y, Liu L, Luo G, Li H, Ma W, Sun L, Wang W, Weng Q, et al. Mesenchymal stem cells therapy improves ovarian function in premature ovarian failure: a systematic review and meta-analysis based on preclinical studies. Front Endocrinol. 2023;14:1165574–1165574.
70. Chen H, Xia K, Huang W, Li H, Wang C, Ma Y, Chen J, Luo P, Zheng S, Wang J, et al. Autologous transplantation of thecal stem cells restores ovarian function in nonhuman primates. Cell Discovery. 2021;7:75–75.
71. Ahmed RH, Galaly SR, Moustafa N, Ahmed RR, Ali TM, Elesawy BH, Ahmed OM, Abdul-Hamid M. Curcumin and mesenchymal stem cells ameliorate ankle, Testis, and Ovary Deleterious histological changes in arthritic rats via suppression of oxidative stress and inflammation. Stem Cells Int. 2021;2021:3516834–3516834.
72. Zhou Y, Yamamoto Y, Xiao Z, Ochiya T. The immunomodulatory functions of mesenchymal Stromal/Stem cells mediated via paracrine activity. J Clin Med. 2019;8:1025.
73. Lai D, Wang F, Dong Z, Zhang Q. Skin-derived mesenchymal stem cells help restore function to ovaries in a premature ovarian failure mouse model. PLoS ONE. 2014;9:e98749–98749.
74. Guzmán A, Hernández-Coronado CG, Gutiérrez CG, Rosales-Torres AM. The vascular endothelial growth factor (VEGF) system as a key regulator of ovarian follicle angiogenesis and growth. Mol Reprod Dev. 2023;90:201–17.
75. Qiu Y, Seager M, Osman A, Castle-Miller J, Bevan H, Tortonese DJ, Murphy D, Harper SJ, Fraser HM, Donaldson LF, Bates DO. Ovarian VEGF(165)b expression regulates follicular development, corpus luteum function and fertility. Reprod (Cambridge England). 2012;143:501–11.
76. Wang J, Liu W, Yu D, Yang Z, Li S, Sun X. Research Progress on the treatment of premature ovarian failure using mesenchymal stem cells: a Literature Review. Front cell Dev Biology. 2021;9:749822–749822.
77. Ding C, Zou Q, Wang F, Wu H, Chen R, Lv J, Ling M, Sun J, Wang W, Li H, Huang B. Human amniotic mesenchymal stem cells improve ovarian function in natural aging through secreting hepatocyte growth factor and epidermal growth factor. Stem Cell Res Ther. 2018;9:55–55.
78. Talele NP, Fradette J, Davies JE, Kapus A, Hinz B. Expression of α-Smooth muscle actin determines the fate of mesenchymal stromal cells. Stem Cell Rep. 2015;4:1016–30.
79. Cho J, Kim TH, Seok J, Jun JH, Park H, Kweon M, Lim JY, Kim GJ. Vascular remodeling by placenta-derived mesenchymal stem cells restores ovarian function in ovariectomized rat model via the VEGF pathway. Lab Invest. 2021;101:304–17.
80. Alarcon-Martinez L, Yilmaz-Ozcan S, Yemisci M, Schallek J, Kılıç K, Can A, Di Polo A, Dalkara T. Capillary pericytes express α-smooth muscle actin, which requires prevention of filamentous-actin depolymerization for detection. Elife 2018, 7.
81. Maacha S, Sidahmed H, Jacob S, Gentilcore G, Calzone R, Grivel JC, Cugno C. Paracrine Mechanisms of Mesenchymal Stromal Cells in Angiogenesis. *Stem Cells Int* 2020, 2020:4356359.
82. Tao H, Han Z, Han ZC, Li Z. Proangiogenic Features of Mesenchymal Stem Cells and Their Therapeutic Applications. *Stem Cells Int* 2016, 2016:1314709.
83. Sheshpari S, Shahnazi M, Ahmadian S, Nouri M, Mesgari Abbasi M, Beheshti R, Rahbarghazi R, Honaramooz A, Mahdipour M. Intra-ovarian injection of bone marrow-derived c-Kit(+) cells for ovarian rejuvenation in menopausal rats. Bioimpacts. 2022;12:325–35.
84. Hirschberg RM, Plendl J, Kaessmeyer S. Alpha smooth muscle actin in the cycling ovary - an immunohistochemical study. Clin Hemorheol Microcirc. 2012;50:113–29.

Publisher's note